Secreted long non-coding RNAs *Gadlor1* and *Gadlor2* aggravate cardiac remodelling during pressure overload by affecting multiple cardiac cell types

Merve Keles[1,2,3]*, Steve Grein[1,3]*, Natali Froese[4], Dagmar Wirth[5], Felix A. Trogisch[1,2,3], Rhys Wardman[1,3], Shruthi Hemanna[1,3], Nina Weinzierl[1], Philipp-Sebastian Koch[6], Stefanie Uhlig[7], Santosh Lomada[3,8], Gesine M. Dittrich[1,3], Malgorzata Szaroszyk[4], Ricarda Haustein[4], Jan Hegermann[9], Abel Martin-Garrido[1], Johann Bauersachs[4], Derk Frank[10, 11], Norbert Frey[3,12], Karen Bieback[7], Julio Cordero[13], Gergana Dobreva[3,13], Thomas Wieland[3,8] and Joerg Heineke[1,2,3]

[1]ECAS (European Center for Angioscience), Department of Cardiovascular Physiology, Medical Faculty Mannheim of Heidelberg University, Mannheim, Germany

[2]CFPM (Core Facility Platform Mannheim), Cardiac Imaging Center, Medical Faculty Mannheim of Heidelberg University, Mannheim, Germany

[3]DZHK (German Center for Cardiovascular Research), partner site Heidelberg/Mannheim, Germany

[4]Department of Cardiology and Angiology, Hannover Medical School, Hannover, Germany

[5]Helmholtz Centre for Infection Research, Model Systems for Infection and Immunity, Braunschweig, Germany

[6]Department of Dermatology, Venereology and Allergology, University Medical Center and Medical Faculty Mannheim, Heidelberg University, Mannheim, Germany

[7]CFPM, FlowCore, Medical Faculty Mannheim of Heidelberg University, Mannheim, Germany

[8]ECAS, Department of Experimental Pharmacology, Medical Faculty Mannheim of Heidelberg University, Mannheim, Germany

[9]Institute of Functional and Applied Anatomy, Core Unit Electron Microscopy, Hannover Medical School, Hannover, Germany

[10]Department of Internal Medicine III, University Hospital Schleswig-Holstein, Kiel, Germany

[11]DZHK, partner site Hamburg/Kiel/Lübeck

[12]Department of Internal Medicine III, Medical Faculty Heidelberg, Heidelberg University, Heidelberg, Germany

[13]ECAS, Department of Cardiovascular Genomics and Epigenomics, Medical Faculty Mannheim of Heidelberg University, Mannheim, Germany

*these authors contributed equally.

Address for Correspondence:

Prof. Dr. Joerg Heineke

European Center for Angioscience (ECAS), Department of Cardiovascular Physiology,

Medical Faculty Mannheim, Heidelberg University

Ludolf-Krehl-Straße 7 – 11, 68167 Mannheim, Germany

Phone: +49 621 383 71850

Email: Joerg.Heineke@medma.uni-heidelberg.de

Short title: *Gadlor1* and *Gadlor2* lncRNAs in Cardiac Remodelling

Abstract

Aims: Pathological overload triggers maladaptive myocardial remodelling that leads to heart failure. Recent studies have shown that long non-coding RNAs (lncRNAs) contribute to the development of cardiac disease. This study investigates two recently discovered and secreted lncRNAs, *Gadlor1* and *Gadlor2* (*Gadlor 1/2*).

Methods and Results: In the heart, *Gadlor 1/2* are mainly expressed in endothelial cells and to a lesser extent in fibroblasts and cardiomyocytes. *Gadlor1/2* are upregulated in failing mouse hearts as well as in the myocardium and serum of heart failure patients. Interestingly, *Gadlor1/2* are secreted from endothelial cells (EC) within extracellular vesicles (EV) and are taken up by cardiomyocytes. *Gadlor* 1/2 knock-out (*Gadlor*-KO) and overexpression during experimental cardiac pressure overload by transverse aortic constriction (TAC) was analysed.

Gadlor-KO mice exhibited reduced cardiomyocyte hypertrophy, enhanced angiogenesis, diminished myocardial fibrosis, and improved cardiac function, but paradoxically suffered from sudden death during prolonged overload. *Gadlor1/2* overexpression, in turn, aggravated hypertrophy, fibrosis and cardiac dysfunction during TAC. Mechanistically, *Gadlor1/2* inhibited angiogenic gene expression in endothelial cells, while promoting the expression of pro-fibrotic genes in cardiac fibroblasts. We employed RNA antisense purification coupled with mass spectrometry (RAP-MS) and identified the calcium/calmodulin-dependent protein kinase type II (CaMKII) as interaction partner of *Gadlor1/2* in cardiomyocytes. By activating CaMKII, *Gadlor1/2* promoted hypertrophic gene-expression and excitation-contraction coupling in these cells. Accordingly, *Gadlor* ablation entailed reduced hypertrophy, but also increased diastolic calcium levels in the cytosol and arrhythmic beating in cardiomyocytes.

Conclusion: *Gadlor1* and *Gadlor2* are novel lncRNAs that are mainly enriched in EC-derived EVs and are upregulated in mouse and human hearts during pathological overload. *Gadlor1/2* affect multiple cardiac cell types and inhibit angiogenesis, induce myocardial fibrosis and hypertrophy as well as alterations in

calcium homeostasis in cardiomyocytes. We suggest that inhibition of *Gadlor* effects in cardiac non-myocytes could be a therapeutic strategy in heart failure.

Key words: Long non-coding RNA – Extracellular vesicles – Heart failure – Hypertrophy – Pressure overload - Calcium/calmodulin-dependent protein kinase type II

Translational Perspective

Here, we characterized two secreted lncRNAs *Gadlor1/2*, which are conserved in humans. We observed increased *Gadlor1/2* levels in human failing myocardium and a negative correlation between *GADLOR2* serum levels and left ventricular ejection fraction in heart failure patients. *Gadlor1/2* ablation in mice reduces cardiac hypertrophy and fibrosis and increases angiogenesis, but slows calcium re-uptake into the sarcoplasmic reticulum (SR) and might thereby trigger arrhythmia and sudden death when cardiac overload persists in the long term. Inhibition of *Gadlor1/2* effects in endothelial cells and fibroblasts, on the other hand, could be beneficial by increasing angiogenesis and reducing fibrosis in the heart.

1. Introduction

Despite recent advances in therapeutic options, chronic heart failure is still one of the leading causes of global mortality, in part due to insufficient means to counteract maladaptive cardiac remodeling.[1-3] Cardiac remodelling comprises global changes in heart shape, reduced function and arrhythmia that are the consequence of cardiomyocyte hypertrophy, altered angiogenesis and myocardial fibrosis.[4, 5,6, 7] The majority of current therapeutic options target protein-coding genes; however, recent studies revealed the significance of non-coding transcripts in cardiovascular development and disease conditions.[5, 8, 9]

Long non-coding RNAs (lncRNAs) are a diverse group of non-coding transcripts that are longer than 200 nucleotides, and that in general do not encode for proteins.[10] Due to their complex structure, lncRNAs can act, for instance, as chromatin modifiers, affect protein functions, or alter mRNA stability or processing.[5] Thereby lncRNAs typically affect gene expression, alternative splicing or signalling pathways.[11, 12] Recent studies have identified several lncRNAs with crucial roles in cardiac remodelling and heart failure.[11, 13-16] Since non-coding transcripts are detectable in human body fluids such as in serum, circulating microRNAs (miRNAs) and lncRNAs are currently being investigated as clinical biomarkers, as well as for being paracrine mediators of cellular communication during stress conditions.[17-19] Intra-myocardial communication is a highly regulated process governing the complex physiology of the heart, whereby proper synchronization is required between cardiomyocytes, endothelial cells (EC) and fibroblasts as the major cardiac cell types.[20, 21] Cellular communication during pathological remodelling can be mediated by proteins, but also by the secretion and transfer of nanoscale extracellular vesicles (microvesicles and exosomes, termed small extracellular vesicles, EVs, in here) that carry non-coding RNAs and alter the behaviour of recipient cells.[22-25,26,27] It is currently emerging that EVs transport lncRNAs between cells and thereby affect endothelial cell function, cardiac fibrosis and hypertrophy, but more work is needed.[23, 25, 28]

Here, we studied two related and secreted lncRNAs *Gadlor1* and *Gadlor2* (GATA-downregulated long non-coding RNA), which are jointly upregulated after endothelial deletion of GATA2.[29] We found that the

expression of both *Gadlor* lncRNAs are significantly increased in hearts of mice after transverse aortic constriction (TAC), but also in the myocardium and serum of patients suffering from chronic heart failure. Moreover, our results revealed that *Gadlor1* and *Gadlor2* are secreted within EVs predominantly by cardiac EC, from which they are mainly taken up by cardiomyocytes, although they also have autocrine/intracrine or paracrine effects on EC and fibroblasts, respectively. In cardiomyocytes, *Gadlor1/2* impact calcium handling, hypertrophy and gene expression, while triggering pro-fibrotic gene expression in fibroblasts and anti-angiogenic effects in EC. Our study reveals that secreted *Gadlor* lncRNAs exhibit heterocellular effects aggravating cardiac remodelling, and that targeted inhibition of *Gadlor1/2* effects particularly in non-myocytes might serve as a novel therapeutic strategy in heart failure.

2. Methods

Detailed descriptions of materials and methods are provided in the **Supplementary Material.**

2.1. Human Samples

Studies on human heart tissue samples were approved by the Institutional Ethical Board of Massachusetts General Hospital (US), where samples were collected from patients with end-stage heart failure undergoing cardiac transplantation.[30] Control heart tissue samples were obtained from healthy organ volunteers when the organ was not eligible for transplantation, or from the victims of traffic accidents. Human serum samples were obtained from healthy blood donors, or from aortic stenosis patients before replacement of the aortic valve (clinical data are available in **Supplementary Table 1**), where all donors were provided a written informed consent for the collection and use of samples, that had received approval from the Institutional Review Board of Christian-Albrechts-Universität Kiel (File number: A174/09).

2.2. Animal Models and Studies

All studies including the use and care of animals were performed ethically with the permission of the Regional Council Karlsruhe and the Lower Saxony State Office for Consumer Protection and Food Safety, Germany. Systemic *Gadlor* knock-out mice (*Gadlor*-KO) were generated by deletion of the respective region of mouse chromosome 16 using a CRISPR-Cas9-based strategy to achieve homozygous deletion. Pressure overload was induced in 8-10 weeks old mice by transverse aortic constriction (TAC) and maintained for 2 weeks for short-term and 8-12 weeks for long-term studies. Mice were monitored with echocardiography before, and during pressure overload studies for assessment of cardiac function.

2.3. Primary Cell Isolation

Isolation of endothelial cells and fibroblasts from adult mouse hearts was performed with MACS-magnetic beads from Miltenyi Biotec based on the manufacturer's protocol. Briefly, the tissue lysate was incubated with CD146 microbeads (Miltenyi Biotec, 130-092-007) before being passed through magnetic columns (Miltenyi Biotec, MS columns 130-042-201) for positive selection of EC. The flow through was incubated with feeder removal microbeads (Miltenyi Biotech, 130-095-531) and eluted after multiple washing steps to collect fibroblasts (FB). Isolation of adult cardiac myocytes was achieved by using a Langendorff perfusion system. Isolated cells were stored as frozen cell pellets for later RNA or protein isolation for corresponding experiments.

2.4. Extracellular Vesicle Isolation

Isolation of EVs was performed with ultracentrifugation from the supernatant of C166 cells that were cultured with EV-depleted FCS. Initially, cell debris and large vesicles (apoptotic bodies) were removed by

centrifugations at 300xg and 10.000xg, respectively. Subsequently, small EVs (including microvesicles and exosomes) were collected with 100.000xg ultracentrifugation for 90 minutes and similarly washed with PBS, before a second round of centrifugation was performed. For details on EV characterization and visualization, see **Supplementary Material.**

2.5. Sarcomere Contractility and Calcium Transient Measurements

Isolated adult cardiomyocytes were plated on laminin coated (10 µg/cm2) 35 mm dishes (MatTek 10 mm Glass bottom dishes, P35G-1.5-10-C) and gently washed 1 hour later with MEM medium without butanedione monoxime (BDM). Contractility and calcium transient measurements were performed by using Ion-Optix Multicell High-throughput (HT) System chamber, where the cells were simultaneously paced (18 V, 2.5 Hz, 4 ms impulse duration), and assessed for sarcomere length and contraction. Calcium handling was recorded after incubation with 1 µM fura-2, AM (Invitrogen, F1221).

2.6. RNA antisense purification coupled with mass spectrometry (RAP-MS)

To identify the protein interaction partners of *Gadlor* lncRNAs we performed RAP-MS. The 5' biotinylated antisense *Gadlor1* and *Gadlor2* probes were pooled in the experiment and the sequences are listed in **Suppl. Table 5**. HL-1 cardiomyocytes overexpressing *Gadlor1* and *Gadlor2* were used, where each experimental group contained three replicates without cross-linking (as a negative control to identify non-specific 'background' proteins) and four replicates with UV cross-linked condition by using 150 mJ/cm^2 of 254 nm UV light. After hybridization of biotin labelled probes, lysates were cleared with streptavidin coated magnetic beads. The captured protein samples were identified by TMT labelling followed by liquid chromatography-mass spectroscopy (LC-MS/MS) by the EMBL Proteomics core facility.

2.7. RNA sequencing and Bioinformatics

RNA isolation was performed from isolated cells as described at indicated time points (2 weeks after TAC or sham surgery). Quality control of RNA samples (Agilent 2100 Fragment Analyser), and library preparation (DNBSEQ Eukaryotic Strand-specific mRNA library) were performed by BGI, Hong Kong. Bulk RNA sequencing from different cardiac cells was performed as stranded and single-end with 50 base sequence read length by BGI with Illumina HiSeq 2500. For details of RNAseq analysis, see **Supplementary Material.**

2.8. Statistical Analysis

Data are shown as mean ± standard error of the mean (SEM). Data analysis and statistical analysis were performed with GraphPad Prism software (Version 8). An unpaired 2-tailed Student t-test was used for comparing 2 groups. Comparing multiple groups for one or multiple conditions was performed with one-way ANOVA and two-way ANOVA, respectively, and Fisher's LSD post-hoc test was conducted when applicable. For non-parametric data sets, the Mann-Whitney and Kruskal-Wallis tests were used to compare two groups and multiple groups, respectively. Values of $p<0.05$ were considered statistically significant.

3. Results

3.1. Increased expression of *Gadlor* lncRNAs in cardiac pressure overload in mice and human failing hearts

Earlier observations by our group had identified two previously unknown lncRNAs *Gadlor1* and *Gadlor2*, which were markedly and jointly upregulated in EC of endothelial-specific GATA2 knock-out mice.[29]

Gadlor1 (AK037972) and *Gadlor2* (AK038629) are located in close proximity to each other on mouse chromosome 16, and are embedded after exon1 of the *Lsamp* (limbic system-associated membrane protein) gene in its intronic region **(Figure 1A)**. *Lsamp* is mainly expressed in the brain, and we did not detect significant *Lsamp* expression in the heart or cardiac EC, and *Lsamp* expression patterns did not change in response to *Gadlor* knock-out in multiple organs **(Supp. Figure 1A-C)**. *Gadlor1* and *Gadlor2* fragments are not matched with any known mouse peptides (BlastP, The National Center for Biotechnology Information (NCBI) database), and we verified that they are non-coding transcripts by using the CPAT algorithm to assess protein-coding probability **(Supp. Figure 1D)**. Cardiac *Gadlor1/2* expression is low in the direct postnatal period but becomes upregulated in the adult (2 months old) heart **(Figure 1B)**. Cellular expression analysis among the main cell types in the heart revealed the highest *Gadlor1* and *Gadlor2* expression in EC, followed by fibroblasts (FB), while the lowest levels were detected in cardiomyocytes (CM) **(Figure 1C)**. In this analysis, *Gadlor* lncRNA levels were also significantly enriched in EC versus whole heart tissue.

Next, we assessed *Gadlor1/2* RNA levels in cardiac disease. Myocardial *Gadlor1 and 2* expression was markedly and jointly upregulated in the chronic phase (12 weeks) after TAC versus sham **(Figure 1D)**. Predominant endothelial expression and the increased abundance during pressure overload were confirmed by fluorescent in situ hybridization **(Supp. Figure 1E-F)**.

The conservation of *Gadlor1/2* RNA between different species was analysed with the EMBOSS-Water platform by assessing the local alignment of human and mouse sequences **(Supp. Figure 2)**. *Gadlor* lncRNAs are highly conserved between human, mouse and rat. Importantly, *GADLOR1/2* expression was also strongly induced in the myocardium of patients suffering from advanced heart failure **(Figure 1E)**, and *GADLOR2* was significantly elevated in the serum of patients with heart failure due to aortic stenosis **(Figure 1F)**. In this patient cohort, high *GADLOR2* levels were found mainly in patients with low left ventricular ejection fraction, and a negative correlation between these two parameters was identified

(Figure 1G). Taken together, these results demonstrate *Gadlor1* and *Gadlor2* as lncRNAs that are co-upregulated in diseased mouse and human hearts.

3.2. *Gadlor* lncRNAs are enriched in EC-derived extracellular vesicles (EVs)

Since *GADLOR2* was detectable in the serum of heart failure patients, and secreted EVs can contain lncRNAs,[23, 26] we hypothesized that *Gadlor*1/2 might be secreted within EVs. To test our hypothesis, the abundance of *Gadlor1/2* was analysed in cultured primary mouse cardiac EC and EVs collected and purified from the supernatant of the EC by ultracentrifugation **(Supp. Figure 3A)**. Initially, we characterized the isolated EVs with electron microscopy (EM), nanoparticle tracking analysis (NTA) and FACS. We found typical microvesicles and exosomes in EM, and the average size of the particles was slightly larger than 100 nm in diameter by NTA, which showed that they were in the range of microvesicles and exosomes (together called as EVs in this study) **(Supp. Figure 3B-C)**. Flow cytometry assessment also confirmed the presence of CD63, CD9 and CD54 as common cell surface markers for EVs **(Supp. Figure 3D)**.

Interestingly, the absolute concentration of *Gadlor1/2* was markedly higher in cardiac EC-derived EVs compared to cardiac EC themselves **(Figure 1H)**. EV *Gadlor1* and *2* RNA levels were not affected by proteinase K (PK), or by RNase A, which indicated *Gadlor1/2* were encapsulated within vesicles and protected from enzyme degradation **(Figure 1I)**. Indeed, *Gadlor* lncRNAs were not protected upon direct incubation with PK and RNase A, or when EVs were dissolved by Triton-X, before RNase A was applied **(Figure 1I)**. In addition to primary cardiac EC, also C166 mouse EC secrete *Gadlor* RNAs in EVs **(Supp. Figure 3E)**. Altogether, these results suggest that *Gadlor1* and *Gadlor2* are highly enriched and encapsulated in EC derived EVs.

3.3. *Gadlor*-KO mice are protected from cardiac dysfunction during cardiac pressure-overload

To investigate the role of *Gadlor* lncRNAs, systemic *Gadlor* knock-out mice (*Gadlor*-KO) were generated by deletion of the whole region of mouse chromosome 16 (including *Gadlor* 1 and 2, since both were consistently jointly regulated in our analyses) by using a CRISPR-Cas9-based strategy **(Figure 1A, Figure 2A)**. Unchallenged *Gadlor*-KO mice were indistinguishable from their wild-type littermates (WT) based on appearance, body weight, heart weight, and baseline echocardiographic analysis **(Supp. Figure 4A-D)**. We detected, however, a mild increase in liver and decrease in brain weight in KO animals compared to WT littermates (**Supp. Figure 4E**).

The ablation of *Gadlor1/2* was confirmed in knock-out animals by qRT-PCR in different organs **(Figure 2B).** We found the highest expression levels of *Gadlor1* and *Gadlor2* in the brain, liver, kidney and as well as in heart compared to other organs in WT animals **(Figure 2B)**. To study the effect of *Gadlor1* and *Gadlor2* in cardiac remodelling during pressure-overload, WT and *Gadlor*-KO animals were subjected to TAC or sham surgery and subsequently monitored for 2 weeks **(Figure 2C)**. The carotid flow was measured after 2 days of TAC in the right and left common carotid arteries to evaluate the strength of the aortic constriction. The RCCA/LCCA (right to left common carotid) artery flow ratio increased to a similar degree in both WT and *Gadlor*-KO animals, indicating comparable pressure overload **(Supp. Figure 4F-G).** We found a significant increase in heart weight to body weight (HW/BW) ratio after 2 weeks of TAC in both WT and *Gadlor*-KO compared to sham animals, however, less hypertrophy (i.e. a reduced HW/BW ratio) was observed in *Gadlor*-KO mice **(Figure 2D)**. Additionally, heart-failure-induced pulmonary congestion was only observed in WT animals after TAC, whereas *Gadlor*-KO animals were protected **(Figure 2E)**. In echocardiography, *Gadlor*-KO mice showed less cardiac systolic dysfunction, a markedly reduced left ventricle wall thickness (LVPW) and less chamber dilation (measured as left end-diastolic volume, LVEDV) compared to WT mice after TAC **(Figure 2F-I)**.

3.4. Deletion of *Gadlor1* and *Gadlor2* alleviates cardiomyocyte hypertrophy and fibrosis *in vivo*

Sirius red staining revealed strongly diminished myocardial fibrosis in *Gadlor*-KO mice, which was supported by reduced cardiac *Col1a1* and *Col3a1* mRNA levels after TAC **(Figure 2J-L).** A lower expression of *Nppa, Nppb*, a lower *Myh7/Myh6* RNA ratio, and a reduced cardiomyocyte cross-sectional confirmed blunted cardiac hypertrophy in *Gadlor*-KO animals compared to WT littermates after TAC **(Figure 2M-O).** Additionally, Isolectin B4 (IB4) staining of capillaries revealed a substantial increase of capillary density in the myocardium of *Gadlor*-KO mice compared to WT animals after TAC **(Figure 2N, P).** Together, our data showed that deletion of *Gadlor*1/2 protected against cardiac hypertrophy, systolic dysfunction, capillary rarefaction and myocardial fibrosis during cardiac pressure overload.

3.5. Overexpression of *Gadlor1* and *Gadlor2* via EVs triggers cardiac dysfunction and fibrosis

To decipher the functional effect of increased *Gadlor1* and *Gadlor2* levels during pressure overload, we administered control EVs and *Gadlor*-enriched EVs to mouse hearts directly before TAC surgery by intra-ventricular injection (and concomitant cross-clamping of the aorta and pulmonary artery distal of the coronary vessels origin). Control EVs were produced by purifying EC-derived EVs from the supernatant of control adenovirus (Ad.β*gal*) infected C166 mouse EC, and *Gadlor1* and *Gadlor2* containing EVs were purified from the supernatant of Ad.*Gadlor1* and Ad.*Gadlor2* infected C166 EC **(Figure 3A)**. We detected significantly higher levels of myocardial *Gadlor1* and *Gadlor2* after 1 week of EV administration **(Figure 3B)**. *Gadlor*-EV treated mice exerted a marked reduction of cardiac systolic function 1 and 2 weeks after TAC, as well as increased wall thickness compared to control EV treated animals (indicated as Cohort I and II **Figure 3A-E**). Histological analyses by Sirius red staining showed exaggerated myocardial fibrosis in *Gadlor*-EV treated mice, which was confirmed by qPCR of *Col1a1* and *Col3a1* mRNA expression in the myocardium **(Figure 3F-G)**. Furthermore, increased expression of *Nppa* and *Nppb*, as well as a trend towards larger cardiomyocyte cross-sectional area verified increased hypertrophic remodelling in *Gadlor*-

EV treated mice **(Figure 3H-J)**. The myocardial capillary density was not changed between experimental groups **(Figure 3K)**.

We concluded that overexpression of *Gadlor1* and *Gadlor2* via administration of endothelial-derived EVs aggravated cardiac dysfunction and hypertrophy, and triggered fibrosis during cardiac pressure overload.

3.6. *Gadlor*-KO mice exert increased mortality during chronic pressure overload

Next, we studied whether the protective effects of *Gadlor1/2* ablation were maintained during persisting long-term pressure overload **(Supp. Figure 5A)**. Similar to our findings after 2 weeks of TAC, *Gadlor*-KO animals had a significantly reduced HW/BW ratio after 8-weeks of TAC compared to WT littermates, an improved systolic left ventricular function with reduced posterior wall thickness, an increased capillary density, diminished cardiac hypertrophy and markedly less fibrosis **(Supp. Figure 5B-J)**. Despite retaining better systolic function and improved remodelling features, we observed a considerably higher mortality rate in *Gadlor*-KO mice starting between two and three weeks after TAC **(Supp. Figure 5K)**. Interestingly, WT and KO animals were indistinguishable in terms of appearance, behaviour and mobility after TAC operation, and death in *Gadlor*-KO mice was unexpected and sudden in nature, possibly due to cardiac arrhythmia.

3.7. *Gadlor1* and *Gadlor2* affect gene expression and angiogenic function in EC

Since EC are the main cardiac cell-type expressing *Gadlor1/2*, and since we observed an increased capillary density in the myocardium of *Gadlor*-KO mice after 2 and 8 weeks of TAC (see above), we performed RNA sequencing from isolated WT and *Gadlor*-KO EC after 2-weeks of TAC. The purity of EC in our MACS-based isolation procedure is >90%.[31] The genome-wide transcriptome analysis via bulk RNAseq identified a total

of 3355 differentially expressed (DE) genes between WT and *Gadlor*-KO, which are shown in the heatmap **(Supp. Figure 6A)**. Gene ontology analysis from DE genes and RT-qPCR revealed and confirmed upregulation of angiogenesis, mitotic cell cycle and respiratory electron transport and downregulation of inflammatory response genes in *Gadlor*-KO EC after 2-weeks TAC **(Supp. Figure 6B-D)**. In addition, myocardial staining for Ki67 as a proliferation marker revealed more Ki67-positive EC in *Gadlor*-KO mice after TAC **(Supp. Figure 6E-F)**. Overexpression of *Gadlor1* and *Gadlor2* by adenovirus in C166 mouse EC showed reduced EC sprouting activity during FGF2 and TGFβ stimulation in comparison to Ad.β*gal* (control) infected cells **(Supp. Figure 6G-H)**. In summary, *Gadlor* lncRNAs exert anti-angiogenic properties in EC.

3.8. Cardiac FBs of *Gadlor*-KO mice induce less fibrosis-associated genes after TAC

Based on our findings, cardiac fibroblasts (FBs) exerted the second highest *Gadlor* lncRNAs expression after EC **(Figure 1C).** To study FB specific gene-expression changes upon *Gadlor* knock-out, we performed bulk RNAseq from isolated cardiac FBs after 2-weeks of TAC. The purity of cardiac FBs in our MACS-based isolation procedure is >90%.[31] Genome-wide analysis revealed a total of 915 downregulated and 998 upregulated genes in *Gadlor*-KO FBs compared to WT mice after TAC, which are shown in a heatmap in **Figure 4A**. Amongst these, we detected a strong downregulation of mainly ECM organization and growth factor associated genes (confirmed by RT-qPCR: *Fgfr1, Igf1, Col1a1, Col3a1, Col6a1*) **(Figure 4B-D)**. Additionally, genes related to the regulation of angiogenesis, blood vessel and endothelium development were upregulated in *Gadlor*-KO FBs, which suggested a contribution of FBs to the enhanced angiogenesis observed in *Gadlor*-KO mice upon overload. The increased expression of *Angpt2, Efna1, Aurkb, Dll1* in cardiac FBs from *Gadlor KO* mice was confirmed by RT-qPCR **(Figure 4C)**. Upon adenoviral overexpression of *Gadlor1* and *Gadlor2* followed with phenylephrine (PE) stimulation, neonatal rat cardiac fibroblasts (NRFB) exerted a decreased expression of *Angpt2*, and an increased expression of *Col1a1* and *Col3a1*, but

no differential expression was observed for *Col4a1* or *Col6a1* **(Figure 4E)**. We concluded that *Gadlor* lncRNAs trigger pro-fibrotic gene expression in cardiac FBs.

3.9. *Gadlor* lncRNAs are transferred to cardiomyocytes via EC-derived EVs

Since *Gadlor1* and *Gadlor2* were mainly secreted by EC, we reasoned that these lncRNAs might exert paracrine effects due to EV-mediated transfer into cardiomyocytes, where they could affect contraction, arrhythmia, or hypertrophy. To analyse whether *Gadlor*1/2 are transferred from EC to cardiomyocytes, we initially overexpressed *Gadlor1/2* by adenovirus in C166 mouse EC, and purified EVs from the supernatant of these cells **(Figure 5A)**. We confirmed the enhancement of *Gadlor1/2* expression in EVs upon *Gadlor1/2* overexpression versus control EC **(Figure 5B)**. The collected EVs were transferred either to neonatal rat cardiomyocytes (NRCMs) or fibroblasts (NRFBs). RT-qPCR analysis showed a significantly higher abundance of *Gadlor1/2* in NRCMs incubated with *Gadlor*-EVs compared to samples incubated with control-EVs or cardiomyocytes without any EV treatment, which indicated that EVs were taken up by cardiomyocytes **(Figure 5C)**. *Gadlor* lncRNAs were also transferred from EC to cardiomyocytes by control EVs, since higher cardiomyocyte *Gadlor1/2* levels were observed after control EV compared to non-EV treatment. Additionally, a mild increase in both *Gadlor1* and *Gadlor2* abundance was also observed in NRFBs after incubation with *Gadlor* EVs, however, at a much lower degree compared to NRCM **(Figure 5C)**. We visualized the uptake of the fluorescently labelled (PKH67) EVs into recipient cardiomyocytes, which was analysed with confocal microscopy after 6 hours and 24 hours **(Figure 5D)**. 3D imaging by confocal Z-stacks confirmed that EVs were internalized into the recipient cardiomyocytes rather than being attached to the surface **(Supp. Video 1)**.

Furthermore, we performed co-culture experiments with isolated *Gadlor*-KO cardiomyocytes (lacking endogenous *Gadlor1/2* expression) and WT mouse cardiac endothelial cells (MCEC, on cell culture inserts)

for 48 hours **(Figure 5E)**. *Gadlor*-KO cardiomyocytes were used to exclude confounding effects of endogenous *Gadlor1/2* expression with exogenous *Gadlor1/2* uptake from EC-derived EVs. As expected, we did not detect any *Gadlor1/2* expression in isolated *Gadlor*-KO cardiomyocytes when they were kept in monoculture, whereas we detected *Gadlor1* and *Gadlor2* after co-culture with WT MCECs **(Figure 5F)**. These results suggested that *Gadlor1/2* were transferred into *Gadlor*-KO cardiomyocytes from MCECs via EV-mediated cell-to-cell transfer. Notably, MCECs that were co-cultured with *Gadlor*-KO cardiomyocytes also exerted an increase of *Gadlor1/2* expression **(Figure 5F)**, which might suggest a possible feedback mechanism between cardiomyocytes and EC.

Sub-cellular fractionation studies to localize *Gadlor* lncRNAs following EV-mediated transfer showed that *Gadlor1* and *Gadlor2* were detected in the cytosol and in a bit higher level in the nucleus of recipient cardiomyocytes **(Figure 5G)**. Overall, endothelial-derived *Gadlor1/2* containing EVs are mainly taken up by cardiomyocytes, where they might act in the cytosol as well as in the nucleus. Cardiac FBs may mainly rely on their own cellular *Gadlor1/2* expression.

3.10. *Gadlor* lncRNAs bind to calcium/calmodulin-dependent protein kinase type II in cardiomyocytes

LncRNAs can interact with proteins to affect their regulatory functions.[32] Even though cardiomyocytes showed the least endogenous levels of *Gadlor* lncRNAs, we still observed strong effects in cardiomyocytes (e.g. reduced hypertrophy) after *Gadlor1/2* deletion upon pressure overload. To decipher this further, we aimed at identifying the binding partners of *Gadlor1/2* in cardiomyocytes by performing RNA antisense purification coupled with mass-spectrometry (RAP-MS) in HL1 cardiac muscle cells after overexpression of *Gadlor1/2* **(Figure 6A)**. Interestingly, we found calcium/calmodulin-dependent protein kinase type II, delta (CaMKIIδ) as the most significant binding partner of *Gadlor1/2* **(Figure 6B)**. Next, we confirmed the

interaction between CaMKII and *Gadlor1/2* with native RNA immunoprecipitation (RIP) followed by qRT-PCR **(Figure 6C)**. Next, we investigated whether Gadlor1/2 could modulate CaMKII function by assessing phospholamban Threonine-17 (Thr17) phosphorylation, which is mediated directly by CaMKII. Indeed, we found reduced and increased Thr17 phospholamban phosphorylation in *Gadlor*-KO mice or *Gadlor*-EV treated mice after TAC, respectively **(Figure 6D-G)**. This indicated that *Gadlor1/2* might promote CaMKII activation in cardiomyocytes.

Since *Gadlor* lncRNAs had interfered in cardiac function, and CaMKII was identified as binding partner, which has a known role in cardiomyocyte excitation-contraction coupling, we investigated cardiomyocyte contractility and calcium dynamics with the CytoCypher High-Throughput (HT) system (Ionoptix) in isolated adult cardiomyocytes after 1-week of TAC. Interestingly, during measurements, a considerably higher number of *Gadlor*-KO cardiomyocytes with arrhythmic behaviour was detected compared to WT cardiomyocytes **(Figure 6H,** example traces are shown in **Supp. Figure 7)**, which indicated that *Gadlor*-KO cardiomyocytes exhibit double contraction even though they were paced with electrical field stimulation, in which each stimulation usually results in a single contraction.

Additionally, while sarcomere shortening and its timing were not significantly affected, cardiomyocyte relaxation was delayed **(Figure 6I)**. Accordingly, *Gadlor*-KO cardiomyocytes displayed a much slower re-uptake of calcium into the sarcoplasmic reticulum (SR), which led to prolonged calcium transients and an increased calcium peak height in *Gadlor*-KO cardiomyocytes **(Figure 6J-K).** Treatment of adult mouse cardiomyocytes with *Gadlor1/2* enriched versus control EC-derived EVs led to augmented, but slower sarcomere shortening, and especially faster cardiomyocyte relaxation **(Figure 6L)**. While calcium peak height and release time were not changed, a faster diastolic calcium re-uptake was detected by a decreased tau value **(Figure 6M)**. Collectively, *Gadlor*-KO myocytes displayed an enhanced propensity to arrhythmic beating, slower diastolic relaxation and slower calcium re-uptake into SR, which entailed increased intercellular calcium levels. Overexpression of *Gadlors1/2,* in turn, led to faster cardiomyocyte

relaxation and faster re-uptake of calcium into the SR. These effects were partially rescued upon KN93 (CaMKII inhibitor) treatment **(Suppl. Figure 8)**, indicating that they might at least in part depend on *Gadlor*1/2 mediated CaMKII activation.

3.11. *Gadlor1* and *Gadlor2* affect cardiomyocyte gene expression

Since *Gadlor1/2* were in part localized in cardiomyocyte nuclei after their transfer **(Figure 5G)**, we hypothesized that they might also affect gene expression in these cells. Comprehensive transcriptome analysis after 2-weeks of TAC between isolated WT and *Gadlor*-KO cardiomyocytes revealed that 2492 genes were up-, while 2956 were downregulated after ablation of *Gadlor1/2* as shown in the heatmap in **Figure 7A**. Functional annotation of DE genes showed that genes related to vasculature development, ECM organization and regulation of cytokine production were upregulated **(Figure 7B)**, while mitochondrial organization, TCA cycle and cardiac muscle contraction genes were downregulated in *Gadlor*-KO cardiomyocytes **(Figure 7B)**. We confirmed the upregulation of *Il6, Tlr9, Col15a1, Col14a1, Adam8* mRNAs, and the downregulation of *Camk2d, Gata4, Actn2, Mfn2* mRNAs in Gadlor-KO cardiomyocytes after TAC by RT-qPCR **(Figure 7C-D)**. To rule out a reduced number of mitochondria as a reason for the downregulation of mitochondrial genes, we assessed the mitochondrial-to-nuclear DNA ratio, but detected no changes in *Gadlor*-KO versus WT mice **(Figure 7E)**. We next assessed the effects of *Gadlor1/2* overexpression on cardiomyocyte gene-expression after PE stimulation. **(Figure 7F)**. This showed that *Gadlor1/2* overexpression in large parts revealed the opposite effects of what was found in *Gadlor*-KO cardiomyocytes, and these effects were partially reversed upon treatment with KN93, indicating CaMKII-dependent effects of *Gadlor1/2* on gene expression.

Comparing the effects of *Gadlor* knock-out in the different cardiac cell types after TAC revealed a strong overlap among upregulated and downregulated genes in FBs, EC and cardiomyocytes **(Suppl. Figure 9)**.

For example, *Gadlor* knock-out led to the upregulation of energy-coupled proton transport mitochondrial genes, actin filament associated genes, and mitotic cell cycle related genes in all three cell types, in addition to the upregulation of cardiac muscle contraction and blood vessel morphogenesis genes in two cell types. On the other hand, genes related to the negative regulation of cell differentiation, cartilage development and the regulation of membrane potential were downregulated in all three cell types, while genes related to cell migration, inflammation, extracellular matrix organization, heart contraction, calcineurin/NFAT signalling and mitochondrial organization were downregulated in at least two of the cell types **(Suppl. Figure 9)**. Therefore, *Gadlor1/2* effects on gene expression contain common, but also unique targets in different cardiac cell types.

4. Discussion

Here, we describe two novel lncRNAs (termed *Gadlor1* and *Gadlor2*) as central regulators of cardiac failure during pressure overload. *Gadlor1* and *Gadlor2* were jointly upregulated in mouse and human failing hearts as well as in the serum of patients with aortic stenosis, where high *GADLOR2* levels were associated with a low ejection fraction. Accordingly, enhanced experimental *Gadlor1/2* expression in mouse hearts triggered aggravated heart failure, myocardial hypertrophy and fibrosis, while combined *Gadlor*-KO mice were protected from cardiac dysfunction, fibrosis and vascular rarefaction during acute and persisting pressure overload. Paradoxically, however, despite retaining better heart function and remodelling features, the complete lack of *Gadlor* lncRNAs during chronic, persisting pressure overload entailed sudden death, most likely due to arrhythmia.

Among the different cell types in the myocardium, we found the highest *Gadlor1/2* expression in EC, where reduced *Gadlor1/2* levels entailed an increased capillary density and cell proliferation after TAC. Importantly, enhanced myocardial angiogenesis was reported to promote cardiac function during pressure

overload.[33, 34] *Gadlor1/2* overexpression in isolated EC reduced angiogenic activity, indicating that *Gadlor* lncRNAs inhibit angiogenic activity in EC in a cell autonomous manner. Because lncRNAs often exert their effects by modifying gene expression, we performed transcriptome profiling by RNA sequencing in cardiac EC after TAC. Indeed, we found that upon *Gadlor1/2* deletion, EC upregulate genes related to angiogenesis, cell cycle and mitosis. Besides this cell-autonomous role, *Gadlor*-KO mice also exerted an increased expression of proangiogenic genes in cardiomyocytes and FBs during TAC, which are both known to affect angiogenesis in a paracrine manner.[33, 35-37]

In addition to EC, cardiac FBs exerted a rather high *Gadlor1/2* expression in the heart, while expression was lower in cardiomyocytes. Transcriptomic profiling in cardiac FBs revealed the downregulation of many extracellular matrix-organizing genes, including pro-fibrotic growth factors, their receptors as well as matrix proteins themselves in *Gadlor*-KO mice. Combined adenoviral overexpression of *Gadlor1* and *Gadlor2* in isolated rat cardiac FB upon phenylephrine (PE) stimulation triggered the opposite effect (i.e. upregulation of matrix genes) for some, but not all of the genes identified by RNA-seq in KO FBs. These data imply that the pro-fibrotic role of *Gadlor1* and *Gadlor2* are mediated by their direct effect on gene expression in cardiac FBs. Increased and decreased fibrosis will likely play a major role in reduced and improved heart function during TAC in mice with enhanced or ablated *Gadlor* expression, respectively.

Remarkably, *Gadlor1/2* are mainly secreted within EVs from EC, which was indicated by a highly enriched *Gadlor* expression in endothelial derived EVs versus EC. This finding indicated a potential paracrine role of *Gadlor* lncRNAs in the heart. Indeed, EVs were reported to contain mainly miRNAs, but also lncRNAs and mRNAs, and to protect these RNA species from degradation by extracellular RNases.[38] EVs might thereby play a role in intercellular communication, especially during stress stimulation or disease, when their production is typically upregulated.[39] In cell culture experiments, we found an effective uptake of *Gadlor1/2* from endothelial-derived EVs in neonatal and adult cardiomyocytes. When adult cardiomyocytes from *Gadlor*-KO mice that naturally could not upregulate intrinsic *Gadlor1/2* lncRNA

expression were co-cultured in the bottom well of a two-chamber system with wild-type EC in the upper well, these effectively restored *Gadlor1/2* levels in the knock-out cardiomyocytes. In addition, the co-cultured EC markedly upregulated their *Gadlor1/2* expression compared to when they were cultured alone. Although we cannot prove this yet *in vivo* in the heart, our results nevertheless indicated a reciprocal intercellular signalling circuit between EC and cardiomyocytes, whereby EC provide *Gadlor* lncRNAs within EVs to cardiomyocytes, which signal back to EC by currently unknown mechanisms to indicate insufficient *Gadlor1/2* levels, when necessary. Indeed, signal responsive EV release had been previously described.[39]

In cardiomyocytes, *Gadlor1/2* lncRNAs are taken up from EC and localize to the cytosolic as well as to the nuclear compartment. Accordingly, we identified CaMKII as a *Gadlor1/2* binding partner in cardiomyocytes, which localizes to both compartments and is activated mainly by calcium/calmodulin, autophosphorylation and oxidation or S-nitrosylation.[40] Its activity is known to be about 3-fold upregulated in failing human hearts.[41] In cardiomyocytes, CaMKII promotes on one hand maladaptive features such as cardiomyocyte hypertrophy and fibrosis by phosphorylating HDAC4, leading to de-repression of MEF2-dependent, pro-hypertrophic gene expression.[42, 43] On the other hand, it has adaptive functions, for example, it promotes calcium re-uptake into the SR by phosphorylating phospholamban at Thr17.[44-46] Because *Gadlor1/2* bind CaMKII and *Gadlor*-KO mice exerted reduced, while *Gadlor*1/2 overexpression led to enhanced Thr17 phosphorylation, we concluded that the *Gadlor* lncRNAs might promote CaMKII activation in a feed-forward loop in cardiomyocytes during pathological overload. Decreased CaMKII activity could account for the improved cardiac remodelling features that we detected in *Gadlor*-KO mice, and at the same time, it slows down calcium re-uptake into the SR, leading to increased cytosolic calcium levels with pro-arrhythmic activity. Indeed, upon *Gadlor1/2* overexpression, pharmacological CaMKII inhibition partially reversed pro-hypertrophic gene expression and reversed increased calcium cycling in isolated cardiomyocytes. With regard to their dichotomous role, *Gadlor1/2* inhibition in cardiomyocytes

might not be a suitable therapeutic strategy during persisting cardiac overload, since although it would lead to inhibition of hypertrophy, there might be the danger of arrhythmia. On the contrary, targeted inhibition of *Gadlor1/2* effects in EC and FB could be beneficial, as it would entail increased angiogenesis and reduced FB-mediated fibrosis, which according to our data are likely the main underlying reasons for improved heart function in *Gadlor*-KO mice. Although more work is needed, we suggest that the inhibition of *Gadlor* effects in cardiac non-myocytes might be a promising strategy to treat heart failure in the future.

Author contributions

M.K designed and performed the experiments, analysed RNAseq data and wrote the first draft of the manuscript. **S.G** designed and performed the experiments and analysed data. **N.F**, **F.A.T**, **R.W**, **S.H, S.L, G.M.D, M.S** and **R.H** performed experiments. **D.W** designed and supervised the generation of *Gadlor*-KO mice. **N.W** maintained the mouse colonies and performed experiments. **P.-S. K., Ja.H, D.F, S.U, K.B, A.M.G** and **J.C** provided experimental support for the study. **No.F., J.B., G.D.** and **T. W.** provide crucial advice for the study and critically revised the paper. **J.H.** designed and conceptualized the study, supervised all the experiments, and prepared the final draft of the manuscript. All authors read and approved the manuscript.

Acknowledgements

The authors thank the Core Facilities Pre-Clinical Models, Live Cell Imaging Mannheim (LIMA) and the Transgenic Mice Service Unit (TGSM) at Helmholtz Centre for Infection Research (HZI) for generating the knockout mice. The authors also acknowledge EMBL Proteomics Core Facility for performing proteomics analysis.

Funding

This study was supported by grants from SFB1366 (CRC1366 - Vascular Control of Organ Function)/ 1-A6 (J.H.) by the Deutsche Forschungsgemeinschaft (DFG).

Disclosures

The following patent has been granted: LncRNAs Gadlor1 and Gadlor2 for use in treating and preventing cardiac remodelling. US11208656 (granted 28.01.2021).

Data Availability

RNA sequencing data sets were deposited in National Center for Biotechnology Information's (NCBI) Gene Expression Omnibus (GEO) repository with the accession number GSE213612.

References

1. Tsao CW, Aday AW, Almarzooq ZI, Alonso A, Beaton AZ, Bittencourt MS, Boehme AK, Buxton AE, Carson AP, Commodore-Mensah Y, Elkind MSV, Evenson KR, Eze-Nliam C, Ferguson JF, Generoso G, Ho JE, Kalani R, Khan SS, Kissela BM, Knutson KL, Levine DA, Lewis TT, Liu J, Loop MS, Ma J, Mussolino ME, Navaneethan SD, Perak AM, Poudel R, Rezk-Hanna M, Roth GA, Schroeder EB, Shah SH, Thacker EL, VanWagner LB, Virani SS, Voecks JH, Wang NY, Yaffe K, Martin SS. Heart Disease and Stroke Statistics-2022 Update: A Report From the American Heart Association. *Circulation* 2022;**145**:e153-e639.
2. Frantz S, Hundertmark MJ, Schulz-Menger J, Bengel FM, Bauersachs J. Left ventricular remodelling post-myocardial infarction: pathophysiology, imaging, and novel therapies. *Eur Heart J* 2022;**43**:2549-2561.
3. Wu X, Reboll MR, Korf-Klingebiel M, Wollert KC. Angiogenesis after acute myocardial infarction. *Cardiovasc Res* 2021;**117**:1257-1273.
4. Frey N, Katus HA, Olson EN, Hill JA. Hypertrophy of the heart: a new therapeutic target? *Circulation* 2004;**109**:1580-1589.
5. Bar C, Chatterjee S, Falcao Pires I, Rodrigues P, Sluijter JPG, Boon RA, Nevado RM, Andres V, Sansonetti M, de Windt L, Ciccarelli M, Hamdani N, Heymans S, Figuinha Videira R, Tocchetti CG, Giacca M, Zacchigna S, Engelhardt S, Dimmeler S, Madonna R, Thum T. Non-coding RNAs: update on mechanisms and therapeutic targets from the ESC Working Groups of Myocardial Function and Cellular Biology of the Heart. *Cardiovasc Res* 2020;**116**:1805-1819.
6. Hill JA, Olson EN. Cardiac plasticity. *N Engl J Med* 2008;**358**:1370-1380.
7. Heineke J, Molkentin JD. Regulation of cardiac hypertrophy by intracellular signalling pathways. *Nat Rev Mol Cell Biol* 2006;**7**:589-600.
8. Huang CK, Kafert-Kasting S, Thum T. Preclinical and Clinical Development of Noncoding RNA Therapeutics for Cardiovascular Disease. *Circ Res* 2020;**126**:663-678.
9. Lu D, Thum T. RNA-based diagnostic and therapeutic strategies for cardiovascular disease. *Nat Rev Cardiol* 2019;**16**:661-674.
10. Wilusz JE, Sunwoo H, Spector DL. Long noncoding RNAs: functional surprises from the RNA world. *Genes Dev* 2009;**23**:1494-1504.
11. Li H, Trager LE, Liu X, Hastings MH, Xiao C, Guerra J, To S, Li G, Yeri A, Rodosthenous R, Silverman MG, Das S, Ambardekar AV, Bristow MR, Gonzalez-Rosa JM, Rosenzweig A. lncExACT1 and DCHS2 Regulate Physiological and Pathological Cardiac Growth. *Circulation* 2022;**145**:1218-1233.
12. Zhao Y, Riching AS, Knight WE, Chi C, Broadwell LJ, Du Y, Abdel-Hafiz M, Ambardekar AV, Irwin DC, Proenza C, Xu H, Leinwand LA, Walker LA, Woulfe KC, Bristow MR, Buttrick PM, Song K. Cardiomyocyte-Specific Long Noncoding RNA Regulates Alternative Splicing of the Triadin Gene in the Heart. *Circulation* 2022;**146**:699-714.
13. Viereck J, Kumarswamy R, Foinquinos A, Xiao K, Avramopoulos P, Kunz M, Dittrich M, Maetzig T, Zimmer K, Remke J, Just A, Fendrich J, Scherf K, Bolesani E, Schambach A, Weidemann F, Zweigerdt R, de Windt LJ, Engelhardt S, Dandekar T, Batkai S, Thum T. Long noncoding RNA Chast promotes cardiac remodeling. *Sci Transl Med* 2016;**8**:326ra322.
14. Han P, Li W, Lin CH, Yang J, Shang C, Nuernberg ST, Jin KK, Xu W, Lin CY, Lin CJ, Xiong Y, Chien H, Zhou B, Ashley E, Bernstein D, Chen PS, Chen HV, Quertermous T, Chang CP. A long noncoding RNA protects the heart from pathological hypertrophy. *Nature* 2014;**514**:102-106.
15. Trembinski DJ, Bink DI, Theodorou K, Sommer J, Fischer A, van Bergen A, Kuo CC, Costa IG, Schurmann C, Leisegang MS, Brandes RP, Alekseeva T, Brill B, Wietelmann A, Johnson CN, Spring-Connell A, Kaulich M, Werfel S, Engelhardt S, Hirt MN, Yorgan K, Eschenhagen T, Kirchhof L, Hofmann P, Jae N, Wittig I, Hamdani N, Bischof C, Krishnan J, Houtkooper RH, Dimmeler S, Boon

RA. Aging-regulated anti-apoptotic long non-coding RNA Sarrah augments recovery from acute myocardial infarction. *Nature communications* 2020;**11**:2039.

16. Micheletti R, Plaisance I, Abraham BJ, Sarre A, Ting CC, Alexanian M, Maric D, Maison D, Nemir M, Young RA, Schroen B, Gonzalez A, Ounzain S, Pedrazzini T. The long noncoding RNA Wisper controls cardiac fibrosis and remodeling. *Sci Transl Med* 2017;**9**.

17. Cheng Y, Wang X, Yang J, Duan X, Yao Y, Shi X, Chen Z, Fan Z, Liu X, Qin S, Tang X, Zhang C. A translational study of urine miRNAs in acute myocardial infarction. *J Mol Cell Cardiol* 2012;**53**:668-676.

18. Kuwabara Y, Ono K, Horie T, Nishi H, Nagao K, Kinoshita M, Watanabe S, Baba O, Kojima Y, Shizuta S, Imai M, Tamura T, Kita T, Kimura T. Increased microRNA-1 and microRNA-133a levels in serum of patients with cardiovascular disease indicate myocardial damage. *Circ Cardiovasc Genet* 2011;**4**:446-454.

19. Schulte C, Barwari T, Joshi A, Zeller T, Mayr M. Noncoding RNAs versus Protein Biomarkers in Cardiovascular Disease. *Trends Mol Med* 2020;**26**:583-596.

20. Sluijter JP, Verhage V, Deddens JC, van den Akker F, Doevendans PA. Microvesicles and exosomes for intracardiac communication. *Cardiovasc Res* 2014;**102**:302-311.

21. Pinto AR, Ilinykh A, Ivey MJ, Kuwabara JT, D'Antoni ML, Debuque R, Chandran A, Wang L, Arora K, Rosenthal NA, Tallquist MD. Revisiting Cardiac Cellular Composition. *Circ Res* 2016;**118**:400-409.

22. Uchida S, Dimmeler S. Long noncoding RNAs in cardiovascular diseases. *Circ Res* 2015;**116**:737-750.

23. Kenneweg F, Bang C, Xiao K, Boulanger CM, Loyer X, Mazlan S, Schroen B, Hermans-Beijnsberger S, Foinquinos A, Hirt MN, Eschenhagen T, Funcke S, Stojanovic S, Genschel C, Schimmel K, Just A, Pfanne A, Scherf K, Dehmel S, Raemon-Buettner SM, Fiedler J, Thum T. Long Noncoding RNA-Enriched Vesicles Secreted by Hypoxic Cardiomyocytes Drive Cardiac Fibrosis. *Mol Ther Nucleic Acids* 2019;**18**:363-374.

24. Piccoli MT, Gupta SK, Viereck J, Foinquinos A, Samolovac S, Kramer FL, Garg A, Remke J, Zimmer K, Batkai S, Thum T. Inhibition of the Cardiac Fibroblast-Enriched lncRNA Meg3 Prevents Cardiac Fibrosis and Diastolic Dysfunction. *Circ Res* 2017;**121**:575-583.

25. Hosen MR, Li Q, Liu Y, Zietzer A, Maus K, Goody P, Uchida S, Latz E, Werner N, Nickenig G, Jansen F. CAD increases the long noncoding RNA PUNISHER in small extracellular vesicles and regulates endothelial cell function via vesicular shuttling. *Mol Ther Nucleic Acids* 2021;**25**:388-405.

26. Bang C, Batkai S, Dangwal S, Gupta SK, Foinquinos A, Holzmann A, Just A, Remke J, Zimmer K, Zeug A, Ponimaskin E, Schmiedl A, Yin X, Mayr M, Halder R, Fischer A, Engelhardt S, Wei Y, Schober A, Fiedler J, Thum T. Cardiac fibroblast-derived microRNA passenger strand-enriched exosomes mediate cardiomyocyte hypertrophy. *J Clin Invest* 2014;**124**:2136-2146.

27. Hosen MR, Goody PR, Zietzer A, Xiang X, Niepmann ST, Sedaghat A, Tiyerili V, Chennupati R, Moore JBt, Boon RA, Uchida S, Sinning JM, Zimmer S, Latz E, Werner N, Nickenig G, Jansen F. Circulating MicroRNA-122-5p Is Associated With a Lack of Improvement in Left Ventricular Function After Transcatheter Aortic Valve Replacement and Regulates Viability of Cardiomyocytes Through Extracellular Vesicles. *Circulation* 2022:101161CIRCULATIONAHA122060258.

28. Huang G, Garikipati VNS, Zhou Y, Benedict C, Houser SR, Koch WJ, Kishore R. Identification and Comparison of Hyperglycemia-Induced Extracellular Vesicle Transcriptome in Different Mouse Stem Cells. *Cells* 2020;**9**.

29. Froese N, Szaroszyk M, Korf-Klingebiel M, Koch K, Schmitto JD, Geffers R, Hilfiker-Kleiner D, Riehle C, Wollert KC, Bauersachs J, Heineke J. Endothelial Cell GATA2 Modulates the Cardiomyocyte Stress Response through the Regulation of Two Long Non-Coding RNAs. *Biology* 2022;**11**:1736.

30. Haq S, Choukroun G, Lim H, Tymitz KM, del Monte F, Gwathmey J, Grazette L, Michael A, Hajjar R, Force T, Molkentin JD. Differential activation of signal transduction pathways in human hearts with hypertrophy versus advanced heart failure. *Circulation* 2001;**103**:670-677.
31. Froese N, Cordero J, Abouissa A, Trogisch FA, Grein S, Szaroszyk M, Wang Y, Gigina A, Korf-Klingebiel M, Bosnjak B, Davenport CF, Wiehlmann L, Geffers R, Riechert E, Jurgensen L, Boileau E, Lin Y, Dieterich C, Forster R, Bauersachs J, Ola R, Dobreva G, Volkers M, Heineke J. Analysis of myocardial cellular gene expression during pressure overload reveals matrix based functional intercellular communication. *iScience* 2022;**25**:103965.
32. Das S, Shah R, Dimmeler S, Freedman JE, Holley C, Lee JM, Moore K, Musunuru K, Wang DZ, Xiao J, Yin KJ, American Heart Association Council on G, Precision M, Council on Arteriosclerosis T, Vascular B, Council on C, Stroke N, Council on Clinical C. Noncoding RNAs in Cardiovascular Disease: Current Knowledge, Tools and Technologies for Investigation, and Future Directions: A Scientific Statement From the American Heart Association. *Circ Genom Precis Med* 2020;**13**:e000062.
33. Heineke J, Auger-Messier M, Xu J, Oka T, Sargent MA, York A, Klevitsky R, Vaikunth S, Duncan SA, Aronow BJ, Robbins J, Crombleholme TM, Molkentin JD. Cardiomyocyte GATA4 functions as a stress-responsive regulator of angiogenesis in the murine heart. *J Clin Invest* 2007;**117**:3198-3210.
34. Oka T, Akazawa H, Naito AT, Komuro I. Angiogenesis and cardiac hypertrophy: maintenance of cardiac function and causative roles in heart failure. *Circ Res* 2014;**114**:565-571.
35. Dittrich GM, Froese N, Wang X, Kroeger H, Wang H, Szaroszyk M, Malek-Mohammadi M, Cordero J, Keles M, Korf-Klingebiel M, Wollert KC, Geffers R, Mayr M, Conway SJ, Dobreva G, Bauersachs J, Heineke J. Fibroblast GATA-4 and GATA-6 promote myocardial adaptation to pressure overload by enhancing cardiac angiogenesis. *Basic Res Cardiol* 2021;**116**:26.
36. Sano M, Minamino T, Toko H, Miyauchi H, Orimo M, Qin Y, Akazawa H, Tateno K, Kayama Y, Harada M, Shimizu I, Asahara T, Hamada H, Tomita S, Molkentin JD, Zou Y, Komuro I. p53-induced inhibition of Hif-1 causes cardiac dysfunction during pressure overload. *Nature* 2007;**446**:444-448.
37. Vidal R, Wagner JUG, Braeuning C, Fischer C, Patrick R, Tombor L, Muhly-Reinholz M, John D, Kliem M, Conrad T, Guimaraes-Camboa N, Harvey R, Dimmeler S, Sauer S. Transcriptional heterogeneity of fibroblasts is a hallmark of the aging heart. *JCI Insight* 2019;**4**.
38. Kim KM, Abdelmohsen K, Mustapic M, Kapogiannis D, Gorospe M. RNA in extracellular vesicles. *Wiley Interdiscip Rev RNA* 2017;**8**.
39. Pironti G, Strachan RT, Abraham D, Mon-Wei Yu S, Chen M, Chen W, Hanada K, Mao L, Watson LJ, Rockman HA. Circulating Exosomes Induced by Cardiac Pressure Overload Contain Functional Angiotensin II Type 1 Receptors. *Circulation* 2015;**131**:2120-2130.
40. Mattiazzi A, Bassani RA, Escobar AL, Palomeque J, Valverde CA, Vila Petroff M, Bers DM. Chasing cardiac physiology and pathology down the CaMKII cascade. *Am J Physiol Heart Circ Physiol* 2015;**308**:H1177-1191.
41. Kirchhefer U, Schmitz W, Scholz H, Neumann J. Activity of cAMP-dependent protein kinase and Ca2+/calmodulin-dependent protein kinase in failing and nonfailing human hearts. *Cardiovasc Res* 1999;**42**:254-261.
42. Backs J, Backs T, Neef S, Kreusser MM, Lehmann LH, Patrick DM, Grueter CE, Qi X, Richardson JA, Hill JA, Katus HA, Bassel-Duby R, Maier LS, Olson EN. The delta isoform of CaM kinase II is required for pathological cardiac hypertrophy and remodeling after pressure overload. *Proc Natl Acad Sci U S A* 2009;**106**:2342-2347.
43. Li C, Cai X, Sun H, Bai T, Zheng X, Zhou XW, Chen X, Gill DL, Li J, Tang XD. The deltaA isoform of calmodulin kinase II mediates pathological cardiac hypertrophy by interfering with the HDAC4-MEF2 signaling pathway. *Biochem Biophys Res Commun* 2011;**409**:125-130.

44. Beckendorf J, van den Hoogenhof MMG, Backs J. Physiological and unappreciated roles of CaMKII in the heart. *Basic Res Cardiol* 2018;**113**:29.
45. Mattiazzi A, Kranias EG. The role of CaMKII regulation of phospholamban activity in heart disease. *Front Pharmacol* 2014;**5**:5.
46. Kemi OJ, Ellingsen O, Ceci M, Grimaldi S, Smith GL, Condorelli G, Wisloff U. Aerobic interval training enhances cardiomyocyte contractility and Ca2+ cycling by phosphorylation of CaMKII and Thr-17 of phospholamban. *J Mol Cell Cardiol* 2007;**43**:354-361.

Figure Legends

Figure 1: *Gadlor* lncRNAs are mainly expressed in cardiac endothelial cells (EC) and their expression is highly increased in mice after pressure-overload and in human failing hearts.

A. Representative scheme of AK037972 *(Gadlor1)* and AK038629 *(Gadlor2)* locus on mouse chromosome 16 and positions of the CRISPR/ Cas9 deletion sites used to generate *Gadlor*-KO mice. **B.** *Gadlor1* and *Gadlor2* expression levels in mouse cardiac tissue from different postnatal developmental stages (P1 – n=5, P5 – n=5, P21 – n=3 and adult (9-weeks old) – n=4), and in **C.** different cardiac cell-types (EC: endothelial cells – n=5, FB: fibroblast – n=6, CM: cardiomyocytes – n=4) and heart tissue (WH: whole heart – n=6). **D.** *Gadlor* lncRNA levels in mouse cardiac tissue after long-term (12 weeks, n=9) TAC (transverse aortic constriction) compared to sham. **E.** *GADLOR1* and *2* expression in control (healthy, n=6) and human failing heart tissue (n=8) samples. **F.** Detection of *GADLOR2* levels (pg/l: picogram/liter) in human serum of healthy volunteers (n=19) and patients with aortic stenosis (n=16). **G.** Correlation analysis of *GADLOR2* levels (pg/l) with ejection fraction (%) of the aortic stenosis patients (n=16) from **F**, (Pearson correlation, Pearson r= -4892 and p-value = 0.0272). **H.** Absolute quantification of total RNA amount of *Gadlor1* and *Gadlor2* in EC and EC-derived EVs (fg/ng: femtogram/ nanogram). **I.** Detection of *Gadlor* lncRNAs in EC-derived EVs treated with proteinase K (PK), RNase or Triton-X as indicated. Data are shown as mean±SEM. Data normality was evaluated with the Shapiro-Wilk test. *P*-values were calculated with Student's t-test for parametric (or Mann-Whitney for non-parametric) for comparing two groups, and one-way ANOVA

was applied for comparing multiple groups followed with Fisher's LSD post-hoc test. *p-value<0.05, **p-value<0.01, ***p-value<0.001, ****p-value<0.0001.

Figure 2: Deletion of *Gadlor* lncRNAs reduces cardiac hypertrophy and fibrosis during cardiac pressure overload.

A. Scheme of *Gadlor*-KO mouse line generation by systemic deletion of the region on chromosome 16 containing both *Gadlor1* and *Gadlor2* by a CRISPR/Cas9 approach. **B.** Assessment of the relative expression of *Gadlor*s in indicated organs in adult WT and *Gadlor*-KO mice (n≥8). The difference in *Gadlor1/2* expression levels between WT and *Gadlor*-KO animals were significant for all organs, in which *Gadlor1* and *Gadlor2* were detected. (Heart: *p-value<0.05, Liver and Kidney: ***p-value<0.001, Brain: ****p-value<0.0001). **C.** Experimental design of TAC operation for *Gadlor*-KO and WT littermates. **D.** Heart weight to body weight ratio (HW/BW, mg/g) and **E.** lung weight (mg) to body weight (g) ratio of *Gadlor*-KO and WT littermates in sham and after 2 weeks TAC (n≥11). **F.** Representative echocardiography images of *Gadlor*-KO and WT mice before (pre-TAC) and after 2 weeks of TAC (2w TAC) shown in parasternal long axis mode, and analysis of **G.** left ventricle (LV) ejection fraction (EF%), **H.** LV posterior wall thickness in diastole (mm) and **I.** LV end diastolic volume (ul), (n≥12). **J.** Representative Sirius-red fibrosis staining in cardiac tissue sections of sham and 2w TAC animals (scale-bar: 1 mm) and **K.** quantification of fibrotic area (n≥4). **L.** Relative mRNA expression of fibrosis marker and **M.** hypertrophy marker genes in heart tissue samples of sham (n=3) and 2w TAC (n=5). **N.** Representative immunofluorescence images of cardiac tissue samples stained with WGA (wheat-germ agglutinin coupled with Alexa Fluor 555) and IB4 (Isolectin B4 coupled with Alexa Fluor 488) in sham and 2-week TAC samples from *Gadlor*-KO and WT littermates, scale-bar: 100 µm. Quantification of **O.** cardiomyocyte cross-sectional area and **P.** myocardial capillary density per cardiomyocyte ratio. Data are shown as mean±SEM. Data normality was evaluated with Shapiro-Wilk test and p-values were calculated with Student's t-test for comparing two groups and two-way ANOVA for

grouped analysis followed with Fisher's LSD post-hoc test. *p-value<0.05, **p-value<0.01, ***p-value<0.001, ****p-value<0.0001.

Figure 3: Overexpression of *Gadlor1* and *Gadlor2* via extracellular vesicles triggers cardiac dysfunction and development of fibrosis after TAC.

A. Scheme of the experimental design depicting the injection of *Gadlor1 and Gadlor2* containing extracellular vesicles for overexpression followed by TAC operation. **B.** Relative expression of *Gadlor1 and Gadlor2* in cardiac tissue samples after 1 week TAC (indicated as cohort I) to validate the overexpression after injection of control (Ad.βgal treated samples, n=5) and *Gadlor*-containing (Ad.*Gadlor1* and Ad.*Gadlor2* treated samples, n=6) EVs. Echocardiographic analysis of **C.** left ventricle (LV) ejection fraction (EF%) after 1 week TAC, and **D.** LV-EF%, **E.** LV posterior wall thickness in diastole (mm) after 2 weeks TAC in mice injected with control EVs and *Gadlor*1 and *Gadlor2* EVs. **F.** Representative images of Sirius-red staining (scale bar: 1 mm) and **G.** quantification of fibrotic area after 2 weeks TAC in mice injected with control EVs and *Gadlor*1 and *2* EVs. **H.** Relative expression of fibrosis marker genes *Col1a1* and *Col3a1* and hypertrophy marker genes *Nppa* and *Nppb* in heart tissue samples of control EV (n=6) and *Gadlor* EVs (n=6) treated mice. **I.** Representative immunofluorescence images of cardiac tissue samples stained with WGA (wheat-germ agglutinin coupled with Alexa Fluor 555) and IB4 (Isolectin B4 coupled with Alexa Fluor 488) in samples from control-EV and *Gadlor*-EV treated animals (scale-bar: 100 µm). Quantification of **J.** cardiomyocyte cross-sectional area and **K.** myocardial capillarization after EV treatment followed by 2 weeks of TAC. Data are shown as mean±SEM. Data normality was evaluated with Shapiro-Wilk test and p-values were calculated with Student's t-test. *p-value<0.05, **p-value<0.01, ***p-value<0.001, ****p-value<0.0001.

Figure 4: RNA sequencing of *Gadlor*-KO cardiac FBs showed less induction of fibrosis-associated genes after TAC.

A. Heatmap showing differentially regulated genes analysed by bulk RNAseq of isolated cardiac fibroblasts after 2-weeks TAC. **B.** Bar plots showing the gene-ontology (GO) analysis of upregulated and downregulated genes in *Gadlor*-KO FBs after 2-weeks TAC (Red: Upregulated in *Gadlor*-KO, Blue: Downregulated in *Gadlor*-KO). Exemplary genes were listed for selected GO-terms. **C-D.** Validation of selected genes from RNAseq data with qRT-PCR in isolated adult cardiac FBs after 2 weeks of TAC (Red: Upregulated in *Gadlor*-KO, Blue: Downregulated in *Gadlor*-KO). **E.** qRT-PCR of selected genes in neonatal rat fibroblasts (NRFB) overexpressing *Gadlor* lncRNAs after *Gadlor1/2* adenovirus treatment (*βgal* as control) followed by phenylephrine (PE) stimulation (100 µM, 24 hours). Data are shown as mean±SEM. Data normality was evaluated with Shapiro-Wilk test and p-values were calculated with Student's t-test for parametric and Mann-Whitney test for non-parametric assessment. *p-value<0.05.

Figure 5: Secreted *Gadlor* lncRNAs are transferred to cardiomyocytes via endothelial-derived EVs.

A. Schematic representation of experimental design of EV (isolated from C166 endothelial cells, EC, supernatant) transfer to NRCMs or NRFBs. **B.** Validation of *Gadlor1* and *Gadlor2* overexpression in isolated EVs. **C.** RT-qPCR detection of *Gadlor1* and *Gadlor2* after transferring control EVs (isolated from Ad*βgal* treated EC) or *Gadlor*-EVs (isolated from Ad*Gadlor1/* 2 treated EC) on neonatal rat cardiomyocytes (NRCMs) or neonatal rat cardiac fibroblasts (NRFBs). The samples were collected after 6 hours of EV incubation. **D.** Visualization of NRCMs that were incubated with PKH67-labelled (green) EVs isolated from C166 EC for 6 hours and 24 hours. Staining was performed with Phalloidin (red) and DAPI (blue). Scale bar: 50 µm. **E.** Scheme of co-culture experiment with transwell (1 µm pore diameter – allows EV transfer). Mouse cardiac EC (MCEC) on top cultured with *Gadlor*-KO cardiomyocytes in the bottom well without

direct cell contact. **F.** RT-qPCR detection of *Gadlor1* and *Gadlor2* in isolated *Gadlor*-KO cardiomyocytes and MCEC mouse EC after 48 hours of mono-culture or co-culture as indicated. **G.** *Gadlor1* and *Gadlor2* expression in the cytosol and nucleus of the recipient NRCMs after EV transfer (as shown in A). Data are shown as mean±SEM. Data normality was evaluated with Shapiro-Wilk test. P-values were calculated with Student's t-test or one-way ANOVA with Fisher's LSD post-hoc test for comparing two or multiple groups, respectively. Two-way ANOVA with Fisher's LSD post-hoc test was applied for grouped analysis when applicable. *p-value<0.05, **p-value<0.01, ***p-value<0.001, ****p-value<0.0001.

Figure 6. *Gadlor* lncRNAs bind to calcium/calmodulin-dependent protein kinase type II in cardiomyocytes.

A. Experimental scheme of RNA-antisense purification coupled with mass spectroscopy (RAP-MS) to identify specific interaction partners of *Gadlor1/2* in HL1 cardiomyocytes treated with βgal and *Gadlor1/2* adenovirus. **B.** Volcano plot indicating the identified interaction partners of *Gadlor1* and *Gadlor2* in cardiomyocytes with RAP-MS (Fold change enrichment (FC) threshold 1.2 and p-value < 0.05). UV crosslinking was used to stabilize protein:RNA interactions and non-crosslinked (N-XL) samples were used as background and removed from crosslinked (XL) samples for each indicated condition. **C.** RNA immunoprecipitation (RIP) performed with anti-IgG or anti-CaMKII antibodies from HL-1 cardiac muscle cell lysate to validate the interaction with *Gadlors*. RT-qPCR analysis showing the enrichment of *Gadlor1* and *Gadlor2* compared to IgG controls. Data was normalized to input RNA expression. (n=3 for each condition) **D-E.** Exemplary Western blots of phospho-Thr17-PLN and total PLN with CSQ as loading control in **(D)** WT and *Gadlor*-KO and **(E)** in control-EV and Gadlor-EV treated mouse heart tissue samples after 2 weeks TAC. **F-G.** Quantification of Western-blots. **H.** Percentage of isolated adult WT and *Gadlor-KO* cardiomyocytes with arrhythmic phenotype after 1-week TAC recorded by Multicell HT system (Ion-Optix) Cell number≥30 in each condition. Sarcomere contractility **(I-K)** and calcium transient **(L-M)** measurements

were recorded in parallel with Multicell HT system with continuous perfusion of basal media on isolated adult cardiomyocytes after 1-week TAC. **I.** Contractility parameters including sarcomere shortening (%) and relaxation. **J.** Calcium parameters including calcium peak height (arbitrary units, AU) and decay time (tau, seconds). **K.** Representative calcium transient recordings of WT and *Gadlor*-KO mice shown as normalized levels of calcium (%). **L.** Sarcomere function and **M.** calcium transient and decay time constant (tau). Recordings were obtained from adult cardiomyocytes isolated from WT mice after 1 week TAC followed by incubation of control-EV (Ad.βgal) and *Gadlor1/2*-EVs (Ad.Gadlor1 and Ad.Gadlor2) for 4-6 hours. Data are shown as mean±SEM. Data normality was evaluated with Shapiro-Wilk test and p-values were calculated with Student's t-test (Mann-Whitney for non-parametric) for comparing two groups. *p-value<0.05, **p-value<0.01, ***p-value<0.001, ****p-value<0.0001.

Figure 7. Deletion of *Gadlor1* and *Gadlor2* affects gene expression in cardiomyocytes.

A. Heatmap showing differentially regulated genes analysed by bulk RNAseq of isolated cardiomyocytes after 2-weeks TAC. **B.** Bar plots showing the gene-ontology (GO) analysis of upregulated and downregulated genes in *Gadlor*-KO cardiomyocytes after 2-weeks TAC. (Red: Upregulated in *Gadlor*-KO, Blue: Downregulated in *Gadlor*-KO). Exemplary genes were listed for selected GO-terms. **C-D.** Validation of selected upregulated and downregulated genes from RNAseq data with qRT-PCR. **E.** Analysis of mitochondrial DNA (mtDNA) to nuclear DNA (nDNA) ratio determined via quantitative PCR by using WT and *Gadlor-KO* heart tissue samples isolated 2-weeks after TAC. Assessment of ND1 and 16S DNA abundance was used to determine the mtDNA/ nDNA ratio. **F.** qRT-PCR of selected genes in HL-1 cardiac muscle cells overexpressing *Gadlor* lncRNAs after *Gadlor1/2* adenovirus treatment (*βgal* as control) followed by phenylephrine (PE) stimulation (100 µM, 24 hours) with and without KN93 (1 µM, 2 hours) addition. Data are shown as mean±SEM. Data normality was evaluated with Shapiro-Wilk test. P-values were calculated with Student's t-test for parametric (or Mann-Whitney for non-parametric) for comparing

1 two groups. Two-way ANOVA with Fisher's LSD post-hoc test was applied for grouped analysis. ns: no

2 significance, *p-value<0.05, **p-value<0.01, ***p-value<0.001, ****p-value<0.0001.

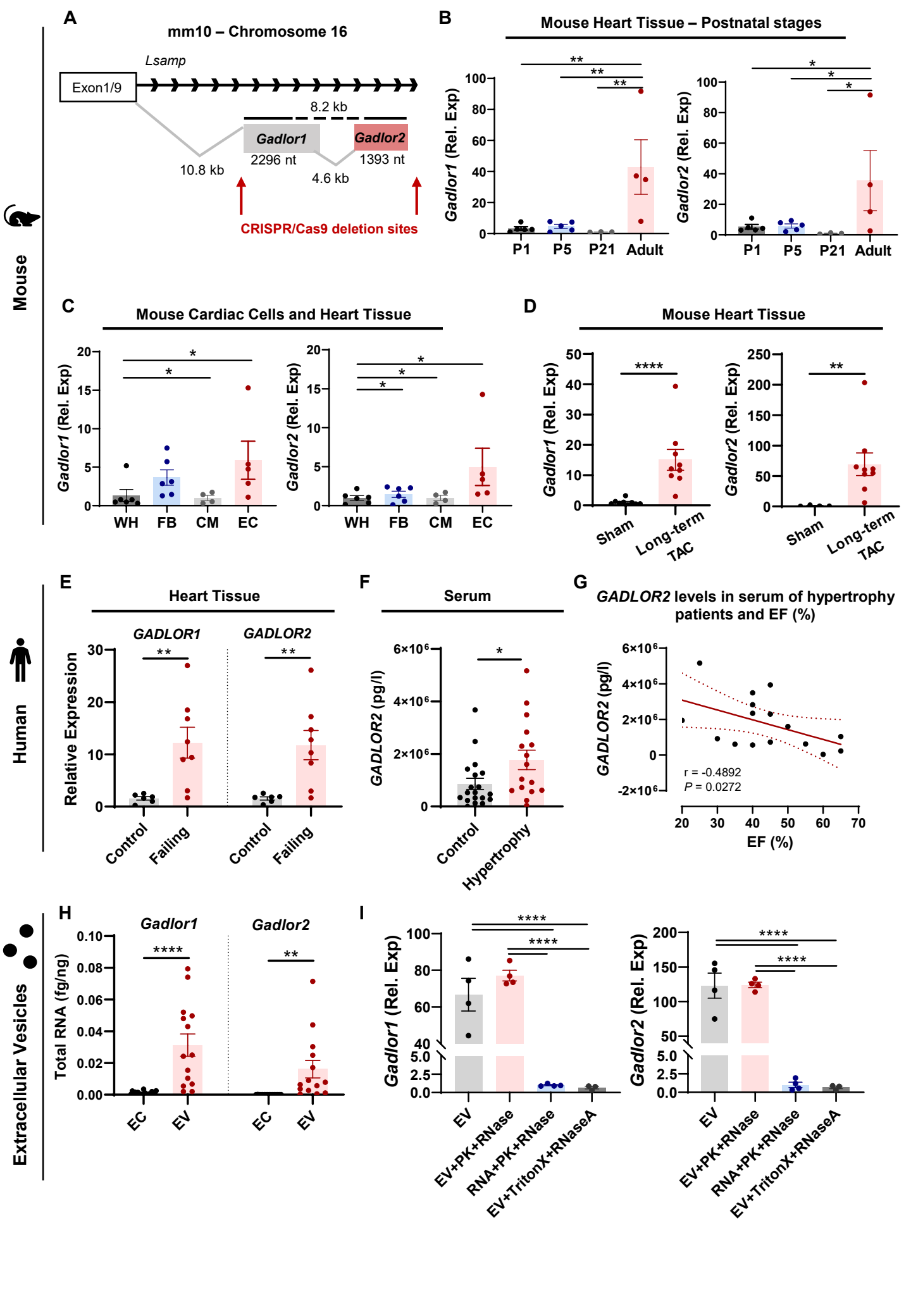
A
mm10 – Chromosome 16
Lsamp
Exon1/9
8.2 kb
Gadlor1
Gadlor2
2296 nt
1393 nt
10.8 kb
4.6 kb
CRISPR/Cas9 deletion sites
B
Mouse Heart Tissue – Postnatal stages
Gadlor1 (Rel. Exp)
Gadlor2 (Rel. Exp)
P1
P5
P21
Adult
Mouse
C
Mouse Cardiac Cells and Heart Tissue
WH
FB
CM
EC
D
Mouse Heart Tissue
Sham
Long-term TAC
Human
E
Heart Tissue
GADLOR1
GADLOR2
Relative Expression
Control
Failing
F
Serum
GADLOR2 (pg/l)
Control
Hypertrophy
G
GADLOR2 levels in serum of hypertrophy patients and EF (%)
GADLOR2 (pg/l)
r = -0.4892
P = 0.0272
EF (%)
Extracellular Vesicles
H
Gadlor1
Gadlor2
Total RNA (fg/ng)
EC
EV
I
Gadlor1 (Rel. Exp)
Gadlor2 (Rel. Exp)
EV
EV+PK+RNase
RNA+PK+RNase
EV+TritonX+RNaseA

Figure 1: *Gadlor* lncRNAs are mainly expressed in cardiac endothelial cells (ECs) and their expression is highly increased in mice after pressure-overload and in human failing hearts.

A. Representative scheme of AK037972 *(Gadlor1)* and AK038629 *(Gadlor2)* locus on mouse chromosome 16 and positions of the CRISPR/ Cas9 deletion sites used to generate *Gadlor*-KO mice. **B.** *Gadlor1* and *Gadlor2* expression levels in mouse cardiac tissue from different postnatal developmental stages (P1 – n=5, P5 – n=5, P21 – n=3 and adult (9-weeks old) – n=4), and in **C.** different cardiac cell-types (EC: endothelial cells – n=5, FB: fibroblast – n=6, CM: cardiomyocytes – n=4) and heart tissue (WH: whole heart – n=6). **D.** *Gadlor* lncRNA levels in mouse cardiac tissue after long-term (12 weeks, n=9) TAC (transverse aortic constriction) compared to sham. **E.** *GADLOR1* and *2* expression in control (healthy, n=6) and human failing heart tissue (n=8) samples. **F.** Detection of *GADLOR2* levels (pg/l: picogram/liter) in human serum of healthy volunteers (n=19) and patients with aortic stenosis (n=16). **G.** Correlation analysis of *GADLOR2* levels (pg/l) with ejection fraction (%) of the aortic stenosis patients (n=16) from **F**, (Pearson correlation, Pearson r= -4892 and p-value = 0.0272). **H.** Absolute quantification of total RNA amount of *Gadlor1* and *Gadlor2* in ECs and EC-derived EVs (fg/ng: femtogram/ nanogram). **I.** Detection of *Gadlor* lncRNAs in EC-derived EVs treated with proteinase K (PK), RNase or Triton-X as indicated. Data are shown as mean±SEM. Data normality was evaluated with the Shapiro-Wilk test. *P*-values were calculated with Student's t-test for parametric (or Mann-Whitney for non-parametric) for comparing two groups, and one-way ANOVA was applied for comparing multiple groups followed with Fisher's LSD post-hoc test. *p-value<0.05, **p-value<0.01, ***p-value<0.001, ****p-value<0.0001.

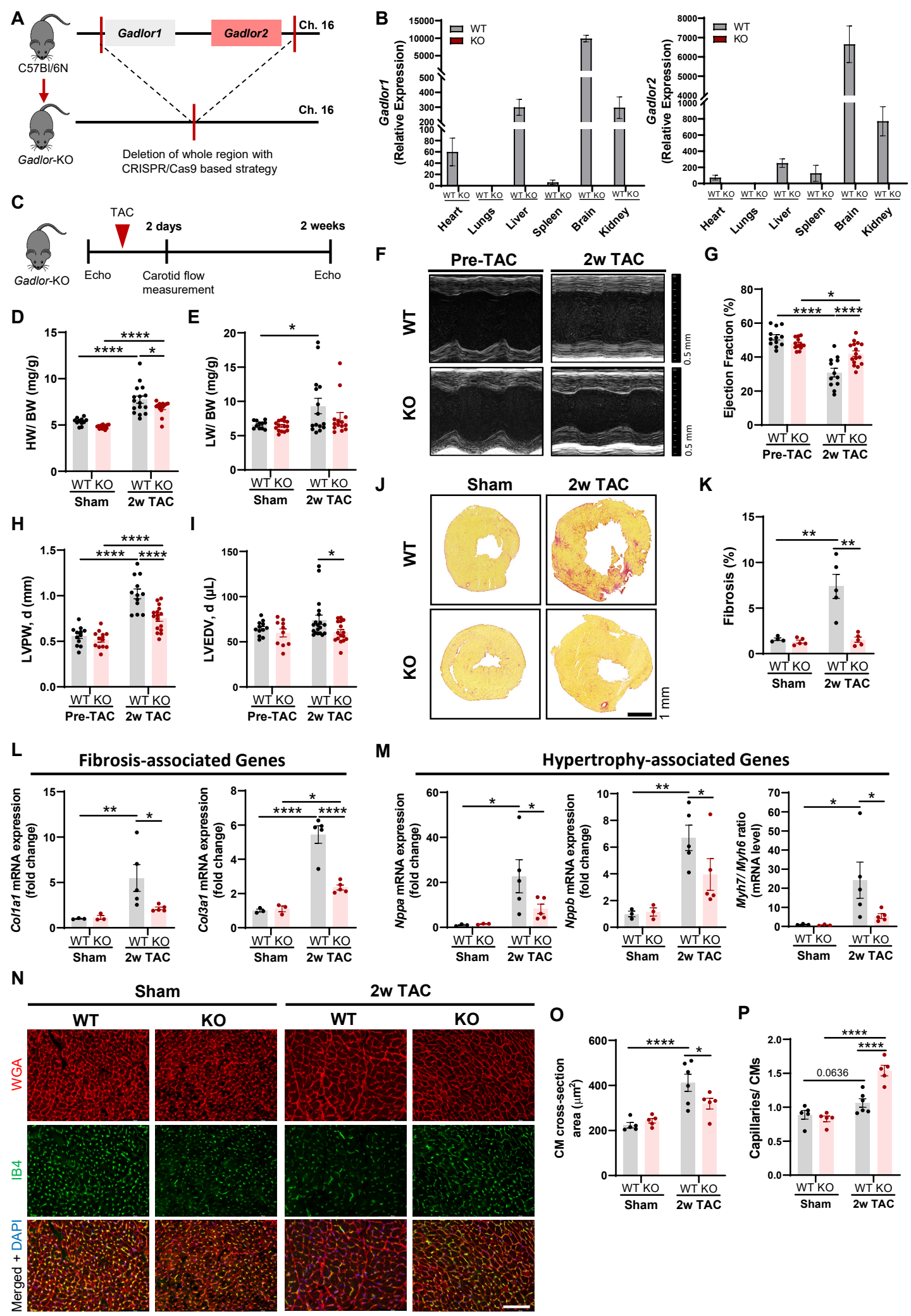
A
C57Bl/6N
Gadlor1
Gadlor2
Ch. 16
Ch. 16
Gadlor-KO
Deletion of whole region with CRISPR/Cas9 based strategy
B
WT
KO
Gadlor1 (Relative Expression)
Gadlor2 (Relative Expression)
Heart
Lungs
Liver
Spleen
Brain
Kidney
C
TAC
2 days
2 weeks
Gadlor-KO
Echo
Carotid flow measurement
Echo
D
HW/ BW (mg/g)
E
LW/ BW (mg/g)
Sham
2w TAC
F
Pre-TAC
2w TAC
WT
KO
0.5 mm
G
Ejection Fraction (%)
Pre-TAC
2w TAC
H
LVPW, d (mm)
I
LVEDV, d (µL)
J
Sham
2w TAC
1 mm
K
Fibrosis (%)
L
Fibrosis-associated Genes
Col1a1 mRNA expression (fold change)
Col3a1 mRNA expression (fold change)
M
Hypertrophy-associated Genes
Nppa mRNA expression (fold change)
Nppb mRNA expression (fold change)
Myh7/ Myh6 ratio (mRNA level)
N
Sham
2w TAC
WT
KO
WGA
IB4
Merged + DAPI
O
CM cross-section area (µm²)
P
Capillaries/ CMs
0.0636

Figure 2: Deletion of *Gadlor* lncRNAs reduces cardiac hypertrophy and fibrosis during cardiac pressure overload.

A. Scheme of *Gadlor*-KO mouse line generation by systemic deletion of the region on chromosome 16 containing both *Gadlor1* and *Gadlor2* by a CRISPR/Cas9 approach. **B.** Assessment of the relative expression of *Gadlor*s in indicated organs in adult WT and *Gadlor*-KO mice (n≥8). The difference in *Gadlor1/2* expression levels between WT and *Gadlor*-KO animals were significant for all organs, in which *Gadlor1* and *Gadlor2* were detected. (Heart: *p-value<0.05, Liver and Kidney: ***p-value<0.001, Brain: ****p-value<0.0001). **C.** Experimental design of TAC operation for *Gadlor*-KO and WT littermates. **D.** Heart weight to body weight ratio (HW/BW, mg/g) and **E.** lung weight (mg) to body weight (g) ratio of *Gadlor*-KO and WT littermates in sham and after 2 weeks TAC (n≥11). **F.** Representative echocardiography images of *Gadlor*-KO and WT mice before (pre-TAC) and after 2 weeks of TAC (2w TAC) shown in parasternal long axis mode, and analysis of **G.** left ventricle (LV) ejection fraction (EF%), **H.** LV posterior wall thickness in diastole (mm) and **I.** LV end diastolic volume (ul), (n≥12). **J.** Representative Sirius-red fibrosis staining in cardiac tissue sections of sham and 2w TAC animals (scale-bar: 1 mm) and **K.** quantification of fibrotic area (n≥4). **L.** Relative mRNA expression of fibrosis marker and **M.** hypertrophy marker genes in heart tissue samples of sham (n=3) and 2w TAC (n=5). **N.** Representative immunofluorescence images of cardiac tissue samples stained with WGA (wheat-germ agglutinin coupled with Alexa Fluor 555) and IB4 (Isolectin B4 coupled with Alexa Fluor 488) in sham and 2-week TAC samples from *Gadlor*-KO and WT littermates, scale-bar: 100 µm. Quantification of **O.** cardiomyocyte cross-sectional area and **P.** myocardial capillary density per cardiomyocyte ratio. Data are shown as mean±SEM. Data normality was evaluated with Shapiro-Wilk test and p-values were calculated with Student's t-test for comparing two groups and two-way ANOVA for grouped analysis followed with Fisher's LSD post-hoc test. *p-value<0.05, **p-value<0.01, ***p-value<0.001, ****p-value<0.0001.

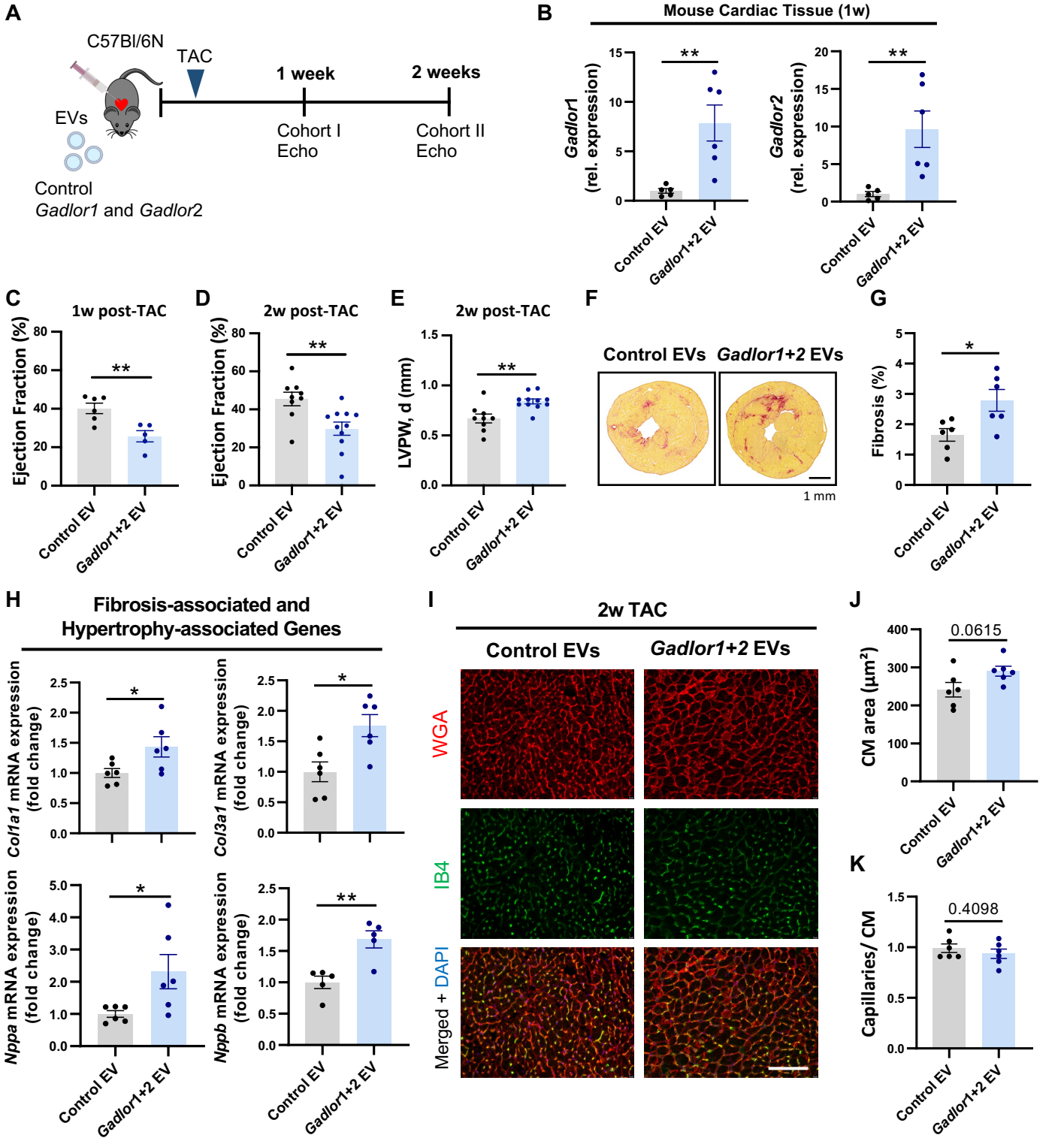

Figure 3: Overexpression of *Gadlor1* and *Gadlor2* via extracellular vesicles triggers cardiac dysfunction and development of fibrosis after TAC.

A. Scheme of the experimental design depicting the injection of *Gadlor1 and Gadlor2* containing extracellular vesicles for overexpression followed by TAC operation. **B.** Relative expression of *Gadlor1 and Gadlor2* in cardiac tissue samples after 1 week TAC (indicated as cohort I) to validate the overexpression after injection of control (Ad.βgal treated samples, n=5) and *Gadlor*-containing (Ad.*Gadlor1* and Ad.*Gadlor2* treated samples, n=6) EVs. Echocardiographic analysis of **C.** left ventricle (LV) ejection fraction (EF%) after 1 week TAC, and **D.** LV-EF%, **E.** LV posterior wall thickness in diastole (mm) after 2 weeks TAC in mice injected with control EVs and *Gadlor*1 and *Gadlor2* EVs. **F.** Representative images of Sirius-red staining (scale bar: 1 mm) and **G.** quantification of fibrotic area after 2 weeks TAC in mice injected with control EVs and *Gadlor*1 and *2* EVs. **H.** Relative expression of fibrosis marker genes *Col1a1* and *Col3a1* and hypertrophy marker genes *Nppa* and *Nppb* in heart tissue samples of control EV (n=6) and *Gadlor* EVs (n=6) treated mice. **I.** Representative immunofluorescence images of cardiac tissue samples stained with WGA (wheat-germ agglutinin coupled with Alexa Fluor 555) and IB4 (Isolectin B4 coupled with Alexa Fluor 488) in samples from control-EV and *Gadlor*-EV treated animals (scale-bar: 100 µm). Quantification of **J.** cardiomyocyte cross-sectional area and **K.** myocardial capillarization after EV treatment followed by 2 weeks of TAC. Data are shown as mean±SEM. Data normality was evaluated with Shapiro-Wilk test and p-values were calculated with Student's t-test. *p-value<0.05, **p-value<0.01, ***p-value<0.001, ****p-value<0.0001.

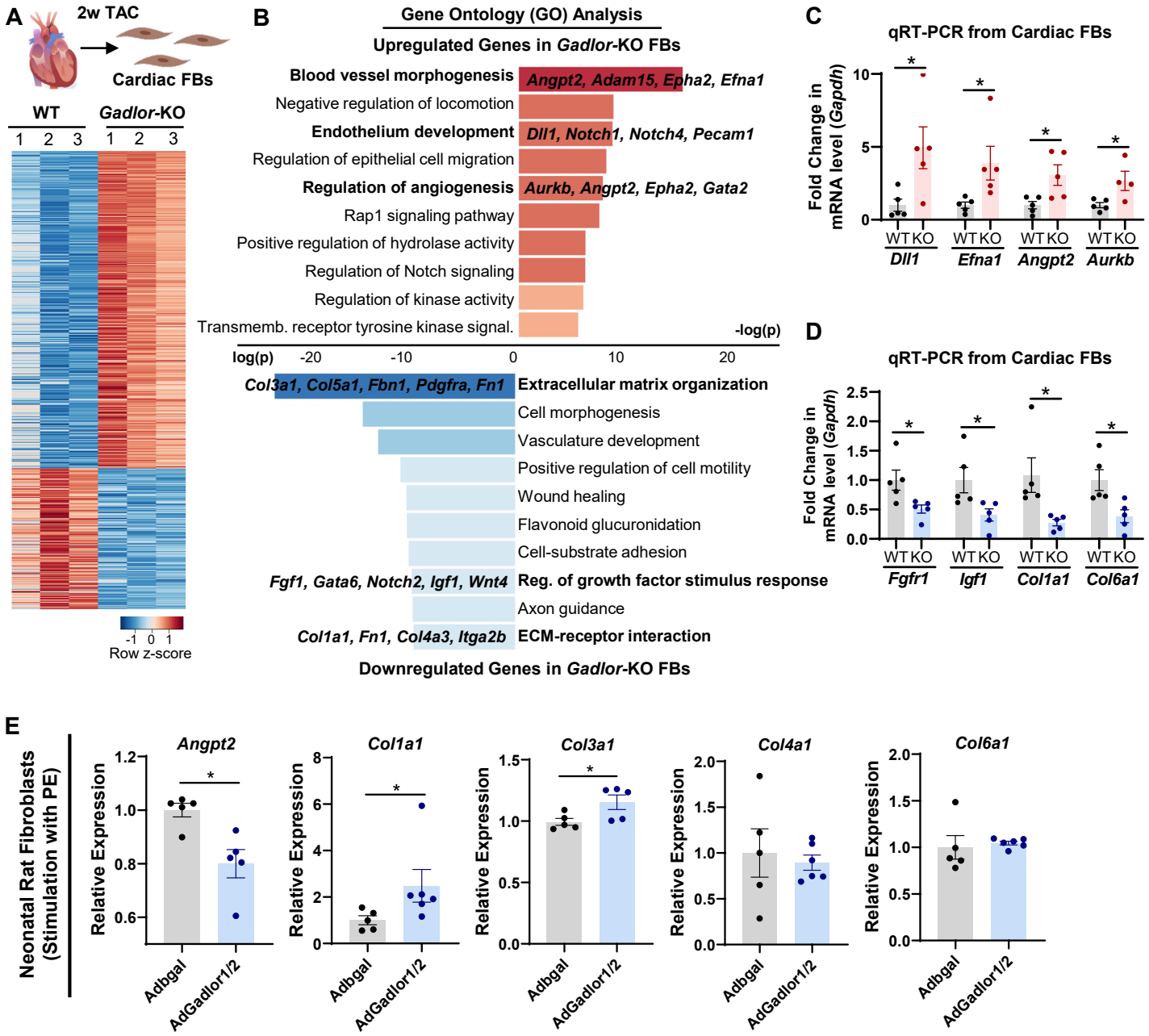

Figure 4: RNA sequencing of *Gadlor*-KO cardiac FBs showed less induction of fibrosis-associated genes after TAC.

A. Heatmap showing differentially regulated genes analysed by bulk RNAseq of isolated cardiac fibroblasts after 2-weeks TAC. **B.** Bar plots showing the gene-ontology (GO) analysis of upregulated and downregulated genes in *Gadlor*-KO FBs after 2-weeks TAC (Red: Upregulated in *Gadlor*-KO, Blue: Downregulated in *Gadlor*-KO). Exemplary genes were listed for selected GO-terms. **C-D.** Validation of selected genes from RNAseq data with qRT-PCR in isolated adult cardiac FBs after 2 weeks of TAC (Red: Upregulated in *Gadlor*-KO, Blue: Downregulated in *Gadlor*-KO). **E.** qRT-PCR of selected genes in neonatal rat fibroblasts (NRFB) overexpressing *Gadlor* lncRNAs after *Gadlor1/2* adenovirus treatment (*βgal* as control) followed by phenylephrine (PE) stimulation (100 µM, 24 hours). Data are shown as mean±SEM. Data normality was evaluated with Shapiro-Wilk test and p-values were calculated with Student's t-test for parametric and Mann-Whitney test for non-parametric assessment. *p-value<0.05.

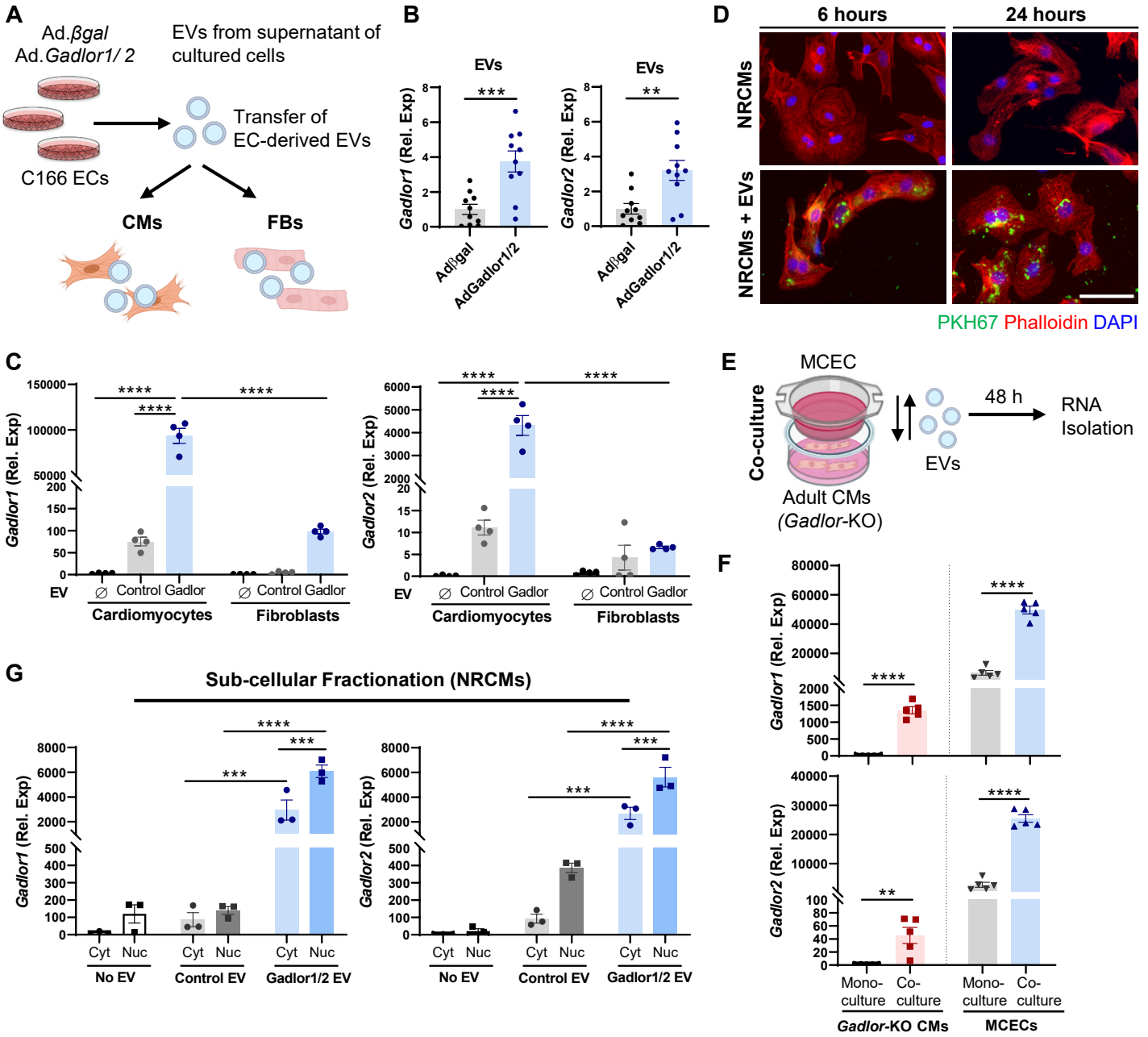

Figure 5: Secreted *Gadlor* lncRNAs are transferred to cardiomyocytes via endothelial-derived EVs.

A. Schematic representation of experimental design of EV (isolated from C166 endothelial cells, EC, supernatant) transfer to NRCMs or NRFBs. **B.** Validation of *Gadlor1* and *Gadlor2* overexpression in isolated EVs. **C.** RT-qPCR detection of *Gadlor1* and *Gadlor2* after transferring control EVs (isolated from Ad*βgal* treated ECs) or *Gadlor*-EVs (isolated from Ad*Gadlor1/* 2 treated ECs) on neonatal rat cardiomyocytes (NRCMs) or neonatal rat cardiac fibroblasts (NRFBs). The samples were collected after 6 hours of EV incubation. **D.** Visualization of NRCMs that were incubated with PKH67-labelled (green) EVs isolated from C166 ECs for 6 hours and 24 hours. Staining was performed with Phalloidin (red) and DAPI (blue). Scale bar: 50 µm. **E.** Scheme of co-culture experiment with transwell (1 µm pore diameter – allows EV transfer). Mouse cardiac EC (MCEC) on top cultured with *Gadlor*-KO CMs in the bottom well without direct cell contact. **F.** RT-qPCR detection of *Gadlor1* and *Gadlor2* in isolated *Gadlor*-KO CMs and MCEC mouse ECs after 48 hours of mono-culture or co-culture as indicated. **G.** *Gadlor1* and *Gadlor2* expression in the cytosol and nucleus of the recipient NRCMs after EV transfer (as shown in A). Data are shown as mean±SEM. Data normality was evaluated with Shapiro-Wilk test. P-values were calculated with Student's t-test or one-way ANOVA with Fisher's LSD post-hoc test for comparing two or multiple groups, respectively. Two-way ANOVA with Fisher's LSD post-hoc test was applied for grouped analysis when applicable. *p-value<0.05, **p-value<0.01, ***p-value<0.001, ****p-value<0.0001.

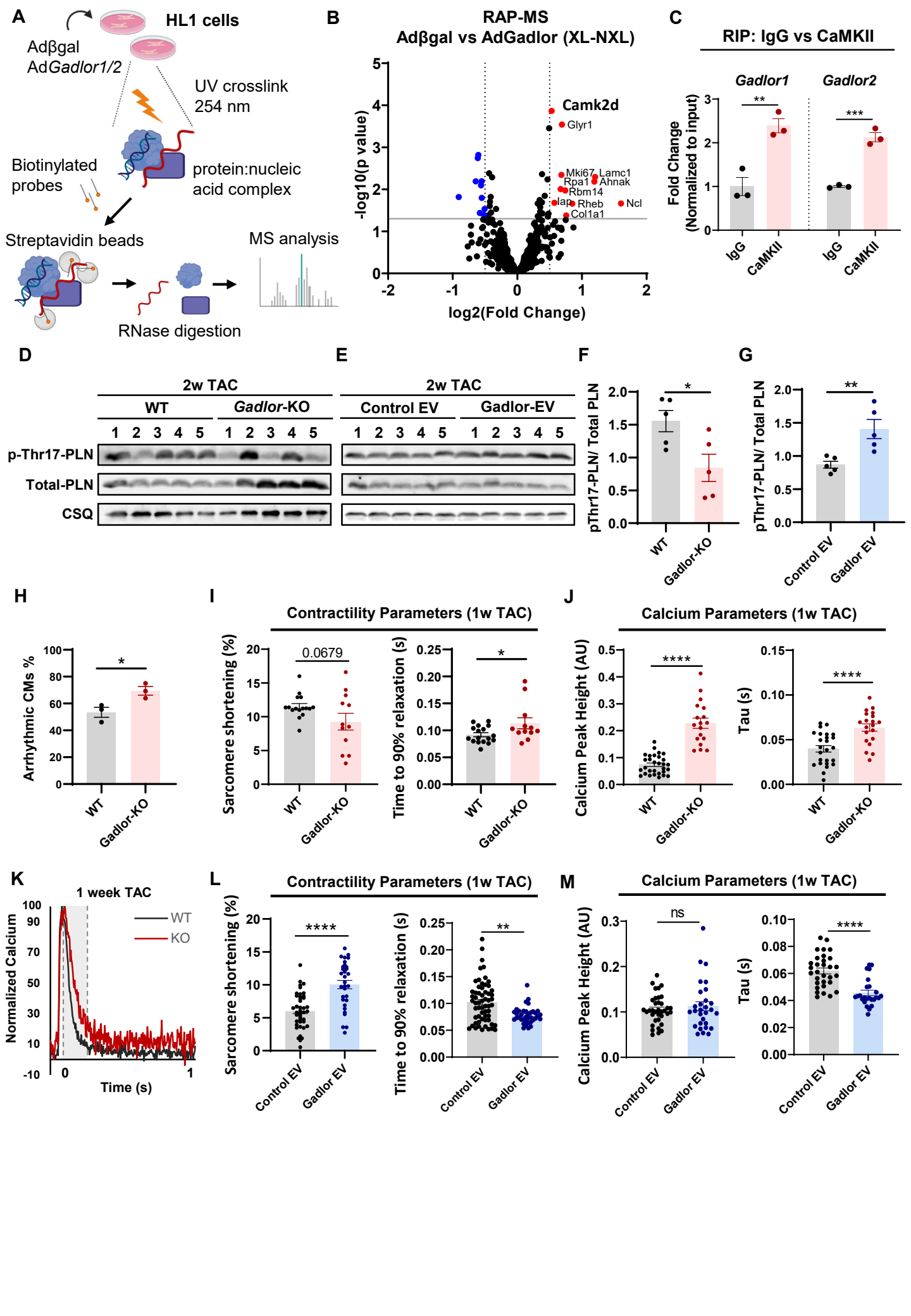
A
HL1 cells
Adβgal
AdGadlor1/2
UV crosslink
254 nm
Biotinylated
probes
protein:nucleic
acid complex
Streptavidin beads
MS analysis
RNase digestion
B
RAP-MS
Adβgal vs AdGadlor (XL-NXL)
Camk2d
Glyr1
Mki67
Lamc1
Rpa1
Ahnak
Rbm14
Iap
Rheb
Ncl
Col1a1
-log10(p value)
log2(Fold Change)
C
RIP: IgG vs CaMKII
Gadlor1
Gadlor2
Fold Change
(Normalized to input)
IgG
CaMKII
D
2w TAC
WT
Gadlor-KO
p-Thr17-PLN
Total-PLN
CSQ
E
2w TAC
Control EV
Gadlor-EV
F
pThr17-PLN/ Total PLN
WT
Gadlor-KO
G
pThr17-PLN/ Total PLN
Control EV
Gadlor EV
H
Arrhythmic CMs %
WT
Gadlor-KO
I
Contractility Parameters (1w TAC)
Sarcomere shortening (%)
0.0679
Time to 90% relaxation (s)
WT
Gadlor-KO
J
Calcium Parameters (1w TAC)
Calcium Peak Height (AU)
Tau (s)
WT
Gadlor-KO
K
1 week TAC
Normalized Calcium
WT
KO
Time (s)
L
Contractility Parameters (1w TAC)
Sarcomere shortening (%)
Time to 90% relaxation (s)
Control EV
Gadlor EV
M
Calcium Parameters (1w TAC)
ns
Calcium Peak Height (AU)
Tau (s)
Control EV
Gadlor EV

Figure 6. *Gadlor* lncRNAs bind to calcium/calmodulin-dependent protein kinase type II in cardiomyocytes.

A. Experimental scheme of RNA-antisense purification coupled with mass spectroscopy (RAP-MS) to identify specific interaction partners of *Gadlor1/2* in HL1 cardiomyocytes treated with βgal and *Gadlor1/2* adenovirus. **B.** Volcano plot indicating the identified interaction partners of *Gadlor1* and *Gadlor2* in cardiomyocytes with RAP-MS (Fold change enrichment (FC) threshold 1.2 and p-value < 0.05). UV crosslinking was used to stabilize protein:RNA interactions and non-crosslinked (N-XL) samples were used as background and removed from crosslinked (XL) samples for each indicated condition. **C.** RNA immunoprecipitation (RIP) performed with anti-IgG or anti-CaMKII antibodies from HL-1 cardiac muscle cell lysate to validate the interaction with *Gadlors*. RT-qPCR analysis showing the enrichment of *Gadlor1* and *Gadlor2* compared to IgG controls. Data was normalized to input RNA expression. (n=3 for each condition) **D-E.** Exemplary Western blots of phospho-Thr17-PLN and total PLN with CSQ as loading control in **(D)** WT and *Gadlor*-KO and **(E)** in control-EV and Gadlor-EV treated mouse heart tissue samples after 2 weeks TAC. **F-G.** Quantification of Western-blots. **H.** Percentage of isolated adult WT and *Gadlor-KO* cardiomyocytes with arrhythmic phenotype after 1-week TAC recorded by Multicell HT system (Ion-Optix) Cell number≥30 in each condition. Sarcomere contractility **(I-K)** and calcium transient **(L-M)** measurements were recorded in parallel with Multicell HT system with continuous perfusion of basal media on isolated adult CMs after 1-week TAC. **I.** Contractility parameters including sarcomere shortening (%) and relaxation. **J.** Calcium parameters including calcium peak height (arbitrary units, AU) and decay time (tau, seconds). **K.** Representative calcium transient recordings of WT and *Gadlor*-KO mice shown as normalized levels of calcium (%). **L.** Sarcomere function and **M.** calcium transient and decay time constant (tau). Recordings were obtained from adult cardiomyocytes isolated from WT mice after 1 week TAC followed by incubation of control-EV (Ad.βgal) and *Gadlor1/2*-EVs (Ad.Gadlor1 and Ad.Gadlor2) for 4-6 hours. Data are shown as mean±SEM. Data normality was evaluated with Shapiro-Wilk test and p-values were calculated with Student's t-test (Mann-Whitney for non-parametric) for comparing two groups. *p-value<0.05, **p-value<0.01, ***p-value<0.001, ****p-value<0.0001.

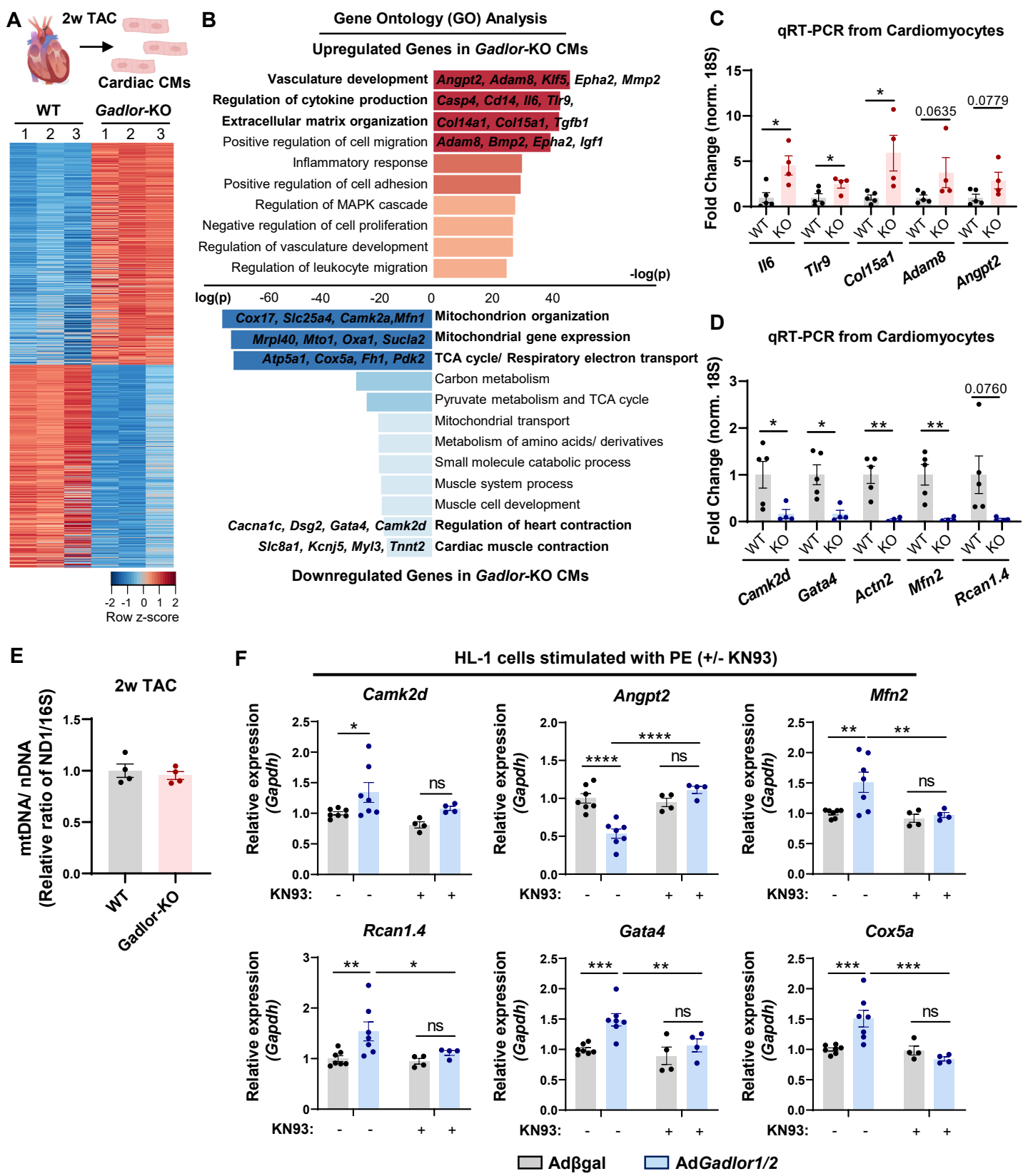

Figure 7. Deletion of *Gadlor1* and *Gadlor2* affects gene expression in cardiomyocytes.

A. Heatmap showing differentially regulated genes analysed by bulk RNAseq of isolated cardiomyocytes after 2-weeks TAC. **B.** Bar plots showing the gene-ontology (GO) analysis of upregulated and downregulated genes in *Gadlor*-KO CMs after 2-weeks TAC. (Red: Upregulated in *Gadlor*-KO, Blue: Downregulated in *Gadlor*-KO). Exemplary genes were listed for selected GO-terms. **C-D.** Validation of selected upregulated and downregulated genes from RNAseq data with qRT-PCR. **E.** Analysis of mitochondrial DNA (mtDNA) to nuclear DNA (nDNA) ratio determined via quantitative PCR by using WT and *Gadlor-KO* heart tissue samples isolated 2-weeks after TAC. Assessment of ND1 and 16S DNA abundance was used to determine the mtDNA/ nDNA ratio. **F.** qRT-PCR of selected genes in HL-1 cardiac muscle cells overexpressing *Gadlor* lncRNAs after *Gadlor1/2* adenovirus treatment (*βgal* as control) followed by phenylephrine (PE) stimulation (100 µM, 24 hours) with and without KN93 (1 µM, 2 hours) addition. Data are shown as mean±SEM. Data normality was evaluated with Shapiro-Wilk test. P-values were calculated with Student's t-test for parametric (or Mann-Whitney for non-parametric) for comparing two groups. Two-way ANOVA with Fisher's LSD post-hoc test was applied for grouped analysis. ns: no significance, *p-value<0.05, **p-value<0.01, ***p-value<0.001, ****p-value<0.0001.